J|A|C|S
ARTICLES
Published on Web 11/26/2002

Highly Selective Binding of Organometallic Ruthenium Ethylenediamine Complexes to Nucleic Acids: Novel Recognition Mechanisms

Haimei Chen, John A. Parkinson, Robert E. Morris, and Peter J. Sadler*

Contribution from the Department of Chemistry, University of Edinburgh, West Mains Road, Edinburgh EH9 3JJ, United Kingdom

Received July 16, 2002; E-mail: p.j.sadler@ed.ac.uk

Abstract: We have investigated the recognition of nucleic acid derivatives by organometallic ruthenium(II) arene anticancer complexes of the type [(η^6-arene)Ru(II)(en)X] where en = ethylenediamine, arene = biphenyl (Bip), tetrahydroanthracene (THA), dihydroanthracene (DHA), *p*-cymene (Cym) or benzene (Ben), X = Cl^- or H_2O using ^1H, ^{31}P and ^{15}N (^{15}N-en) NMR spectroscopy. For mononucleosides, {(η^6-Bip)Ru(en)}$^{2+}$ binds only to N7 of guanosine, to N7 and N1 of inosine, and to N3 of thymidine. Binding to N3 of cytidine was weak, and almost no binding to adenosine was observed. The reactivity of the various binding sites of nucleobases toward Ru at neutral pH decreased in the order G(N7) > I(N7) > I(N1), T(N3) > C(N3) > A(N7), A(N1). Therefore, pseudo-octahedral diamino Ru(II) arene complexes are much more highly discriminatory between G and A bases than square-planar Pt(II) complexes. Such site-selectivity appears to be controlled by the en NH_2 groups, which H-bond with exocyclic oxygens but are nonbonding and repulsive toward exocyclic amino groups of the nucleobases. For reactions with mononucleotides, the same pattern of site selectivity was observed, but, in addition, significant amounts of the 5′-phosphate-bound species (40−60%) were present at equilibrium for 5′-TMP, 5′-CMP and 5′-AMP. In contrast, no binding to the phosphodiester groups of 3′, 5′-cyclic-GMP (cGMP) or cAMP was detected. Reactions with nucleotides proceeded via aquation of [(η^6-arene)Ru(en)Cl]$^+$, followed by rapid binding to the 5′-phosphate, and then rearrangement to give N7, N1, or N3-bound products. Small amounts of the dinuclear species, e.g., Ru-*O*(PO_3)GMP*N7*−Ru, Ru-*O*(PO_3)IMP*N1*−Ru, Ru-*O*(PO_3)TMP*N3*−Ru, Ru-*N7*IMP*N1*−Ru, and Ru-*N7*Ino*N1*−Ru were also detected. In competitive binding experiments for [(η^6-Bip)Ru(en)Cl]$^+$ with 5′-GMP versus 5′-AMP or 5′-CMP or 5′-TMP, the only final adduct was [(η^6-Bip)Ru(en)(*N7*-GMP)]. Ru−H_2O species were more reactive than Ru−OH species. The presence of Cl^- or phosphate in neutral solution significantly decreased the rates of Ru−N7 binding through competitive coordination to Ru. In kinetic studies (pH 7.0, 298 K, 100 mM $NaClO_4$), the rates of reaction of cGMP with {(η^6-arene)Ru(II)(en)X}$^{n+}$ (X = Cl^- or H_2O) decreased in the order: THA > Bip > DHA ≫ Cym > Ben, suggesting that N7-binding is promoted by favorable arene-purine hydrophobic interactions in the associative transition state. These findings have revealed that the diamine NH_2 groups, the hydrophobic arene, and the chloride leaving group have important roles in the novel mechanism of recognition of nucleic acids by Ru arene complexes, and will aid the design of more effective anticancer complexes, as well as new site-specific DNA reagents.

Introduction

Studies of the molecular recognition of DNA and RNA are of fundamental importance in post-genomic chemistry. The rational design of new DNA-binding agents that recognize specific sequences or structures, and can modify specific DNA functions such as replication and transcription, provides an effective approach for development of novel chemotherapeutic anticancer drugs.[1] Noncovalent interactions play key roles in biological molecular recognition.[2] Metal coordination, combined with, for example, hydrogen bonding, hydrophobic and electrostatic interactions, can effectively enhance site- and base-selective recognition of nucleic acids. Selective coordination to nucleobases is influenced by structural and electronic factors arising from the nucleobase and the complex itself.[3] Both hydrogen-bonding and nonbonding repulsive interactions between the exocyclic groups on the bases and the chelate ligands in metal complexes can lead to selective reactions. Hydrophobic interactions can increase DNA affinity and give rise to highly specific recognition of DNA base sequences.[4] Zn(II) macrocyclic tetraamine (1,4,7,10-tetraazacyclododecane, cyclen) complexes with quinolyl or naphthyl pendants selectively bind to AT-rich regions of DNA mainly via Zn(II)-N(3)(thymine) coordination,[5]

(1) (a) Chaires, J. B. *Curr. Opin. Struct. Biol.* **1998**, 314−320. (b) Jenkins, T. C. *Curr. Med. Chem.* **2000**, *7*, 99−115.
(2) (a) Müller-Dethlefs, K.; Hobza, P. *Chem. Rev.* **2000**, *100*, 143−167. (b) *Comprehensive Supramolecular Chemistry*; Lehn, J.-M., Atwood, J. L., Davies, J. E. D., MacNicol, D. D., Vögtle, F., Eds.; Pergamon: Oxford, 1996.
(3) (a) Martin, R. B. *Acc. Chem. Res.* **1985**, *18*, 32−38. (b) Marzilli, L. G.; Kistenmacher, T. J. *Acc. Chem. Res.* **1977**, *10*, 146−152.
(4) Erkkila, K. E.; Odom, D. T.; Barton, J. K. *Chem. Rev.* **1999**, *99*, 2777−2795.

whereas incorporation of anthraquinone pendants into the cyclen ring allows recognition of G bases via a dominant $\pi-\pi$ stacking interaction.[6] There is precedent for incorporating potential DNA intercalators into metal anticancer complexes. Examples include $[Pt(AO)\text{-}(CH_2)_6\text{-}(en)Cl_2]^+$, *cis*-$[Pt(NH_3)_2(N9\text{-}AA)]$ (AO = acridine orange; *N9*-AA = 9-aminoacridine),[7,8] and *trans*-$[PtCl_2(NH_3)L]$ (L = planar aromatic N donor such as pyridine, thiazole, or quinoline),[9] where the additional intercalation or hydrophobic interaction after covalent binding of the Pt to nucleobases can lead to enhanced activity.

We have found that organometallic ruthenium(II) complexes of the type $[(\eta^6\text{-arene})RuCl(X)(Y)]$ (X, Y are monodentate or chelating ligands) are cytotoxic to cancer cells, including cisplatin-resistant cell lines. Preliminary structure−activity data have shown that compounds are active when X, Y belong to a chelating diamine such as ethylenediamine (en) or its derivatives containing NH groups in the amine. The complex $[(\eta^6\text{-Bip})Ru(en)Cl][PF_6]$ is active in vivo against the A2780 xenograft model of human ovarian cancer, and is also active against A2780cis, the cisplatin-resistant xenograft.[10] The cytotoxicity increases with increase in size of the η^6-arene. For example, complexes which contain η^6-tetra- or di-hydroanthracene rings (THA, DHA) or biphenyl (Bip) have much higher activities than compounds containing a single ring such as η^6-benzene (Ben) or η^6-cymene (Cym).[10,11] A potential target for these organometallic Ru(II) complexes is DNA, and the preferred binding site appears to be guanine.[11] We have studied the structures of guanine adducts of THA, DHA, and Bip complexes and found stereospecific hydrogen-bonding of en NH with G O6, and strong arene-nucleobase stacking, both in the solid state by X-ray crystallography, and in solution by NMR methods.[12,13] These studies have revealed several DNA recognition features and suggested a potential DNA-binding mode, involving simultaneous intercalation and covalent coordination. The diamine NH group and hydrophobic arene group as well as the Cl leaving group may therefore all play important roles in the anticancer activity.

It is now important to understand how stereospecific hydrogen-bonding can lead to specific DNA site-recognition and whether arene−purine hydrophobic interactions influence the kinetics of DNA binding. Therefore, we have studied both the thermodynamics and kinetics of the binding of $[(\eta^6\text{-arene})Ru(en)X]^{n+}$ complexes (arene = tetra-, di-hydroanthracene (THA, DHA), biphenyl (Bip), *p*-cymene (Cym) and benzene (Ben); X = Cl or H_2O) to mononucleotides and mononucleosides (G, I, A, C, and T) using ^1H, ^{31}P, ^{15}N (^{15}N-en) NMR spectroscopy, together with pH titrations. These studies show that these novel organometallic ruthenium ethylenediamine anticancer complexes are highly selective in their recognition of nucleic acid bases and that the nature of the coordinated arene has a dramatic effect on the kinetics of binding. Such insights can direct new synthetic work for optimization of drug activity.

Chart 1. Structures and Atom Numbering for Nucleobases and Their Derivatives.

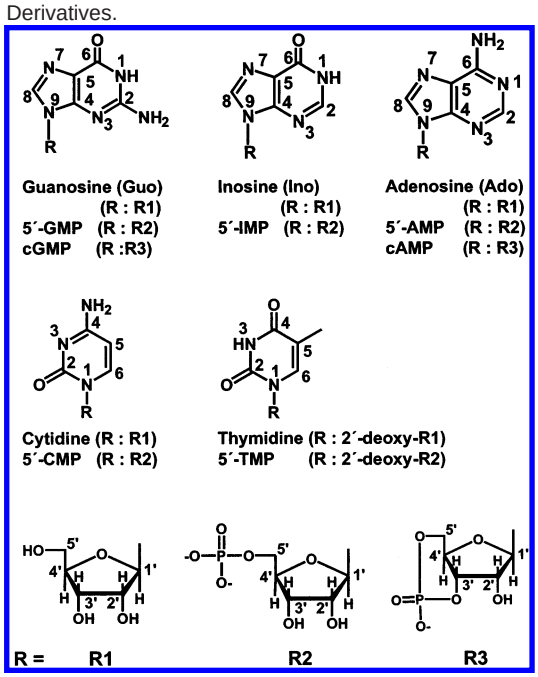

Chart 2. Arene Complexes Studied in This Work

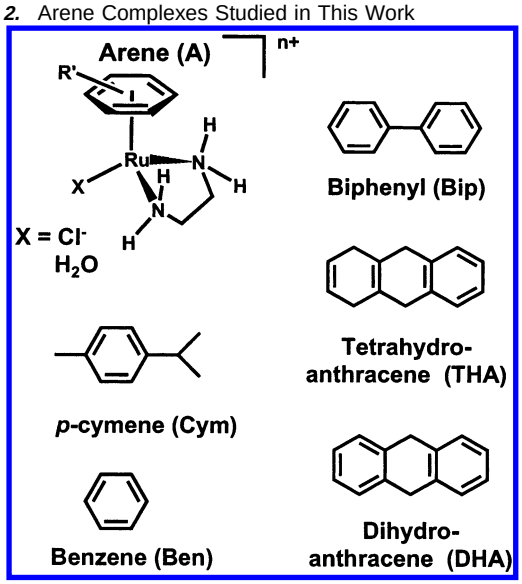

Experimental Section

Materials. Chloro complexes $[(\eta^6\text{-arene})Ru(en)Cl][PF_6]$ (arene = Bip, THA, DHA, Cym, and Ben, Chart 2) were synthesized as described previously.[11,12] The mono-nucleotides 5′-GMP, 3′-GMP, 3′, 5′-cyclic GMP, 5′-IMP, 5′-AMP, 3′, 5′-cyclic AMP, 5′-CMP, and 5′-TMP (all as sodium salts), and the nucleosides guanosine, inosine, adenosine, cytidine, and thymidine were purchased from Sigma or Aldrich. The purity was checked by ^1H and ^{31}P NMR spectroscopy. D_2O (99.98%) was obtained from Aldrich. All NMR experiments were performed in 10% D_2O/90% H_2O.

(5) Kikuta, E.; Murata, M.; Katsube, N.; Koike, T.; Kimura, E. *J. Am. Chem. Soc.* **1999**, *121*, 5426−5436.
(6) Kikuta, E.; Matsubara, R.; Katsube, N.; Koike, T.; Kimura, E. *J. Inorg. Biochem.* **2000**, *82*, 239−249.
(7) Bowler, B. E.; Ahmed, K. J.; Sundquist, W. I.; Hollis, L. S.; Whang, E. E.; Lippard, S. J. *J. Am. Chem. Soc.* **1989**, *111*, 1299−1306.
(8) Sundquist, W. I.; Lippard, S. J. *Coord. Chem. Rev.* **1990**, *100*, 293−322.
(9) (a) Farrell, N.; Ha, T. T. B.; Souchard, J.-P.; Wimmer, F. L.; Cros, S.; Johnson, N. P. *J. Med. Chem.* **1989**, *32*, 2240−2241. (b) Farrell, N. *Met. Ions Biol. Syst.* **1996**, *32*, 603−639. (c) Bierbach, U.; Qu, Y.; Hambley, T. W.; Peroutka, J.; Nguyen, H. L.; Doedee, M.; Farrell, N. *Inorg. Chem.* **1999**, *38*, 3535−3542. (d) Zákovská, A.; Nováková, O.; Balcarová, Z.; Bierbach, U.; Farrell, N.; Brabec, V. *Eur. J. Biochem.* **1998**, *254*, 547−557.
(10) Aird, R. E.; Cummings, J.; Ritchie, A. A.; Muir, M.; Morris, R. E.; Chen, H.; Sadler, P. J.; Jodrell, D. I. *Brit. J. Cancer* **2002**, *86*, 1652−1657.
(11) Morris, R. E.; Aird, R. E.; Murdoch, P. del S.; Chen. H.; Cummings, J.; Hughes, N. D.; Parsons, S.; Parkin, A.; Boyd, G.; Jodrell, D. I.; Sadler, P. J. *J. Med. Chem.* **2001**, *44*, 3616−3621.
(12) Chen, H.; Parkinson, J. A.; Parsons, S.; Coxall, R. A.; Gould, R. O.; Sadler, P. J. *J. Am. Chem. Soc.* **2002**, *124*, 3064−3082.
(13) A similar G C6O···HN H-bond is present in the X-ray structure of $[(\eta^6\text{-benzene})Ru(L\text{-Ala})(9EtG)]Cl\cdot 2H_2O$: Sheldrick, W. S.; Heeb, S. *Inorg. Chim. Acta* **1990**, *168*, 93−100.

Scheme 1. Reaction of $[(\eta^6\text{-Bip})\text{Ru(en)Cl}]^+$ with 5′-GMP (5 mM, 1:1) in Aqueous Solution at pH = 7.15, 298 K[a]

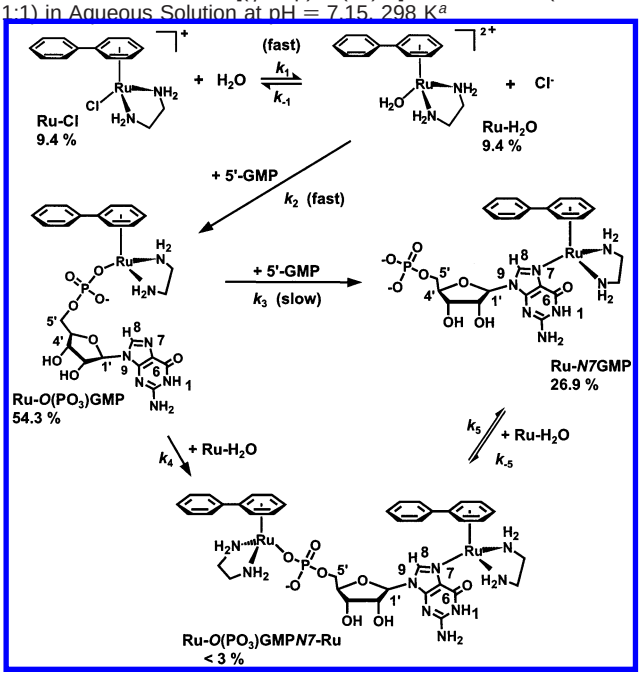

[a] Species distribution (%) is shown after 55 min reaction, and is based on $^{15}NH_2$-en ^{1}H NMR intensities (except for the dinuclear species which was based on H8 intensities). The intermediate Ru−O−*O*(PO_3)GMP (peak b) formed during the reaction mixing time, slowly rearranged into Ru−*N7*GMP (peak c), and then eventually disappeared after 22 h (see Figure 1A). The intermediate Ru−*O*(PO_3)GMP*N7*−Ru (peak d) was evident after 2 h, and eventually disappeared after 22 h; it persisted if Ru was present in excess. When more Ru−Cl (50%) was added to the final mixture, more of species d (30%) formed after 24 h at 310 K.

Preparation of Aqua Ru(arene) Complexes. An aliquot of a 100 mM aqueous solution of $AgNO_3$ (0.98 mol equiv) was added to a solution of $[(\eta^6\text{-arene})\text{Ru(en)Cl}][PF_6]$, giving a yellow-orange solution and an immediate precipitate of AgCl. This mixture was kept at ambient temperature overnight (protected from light) and was then filtered to remove AgCl. The resulting yellow solutions[14] were used freshly and directly for reactions with 5′-GMP and cGMP.

pH Titrations. For the reaction of $[(\eta^6\text{-Bip})\text{Ru(en)Cl}]^+$ (12 mM) with 5′-GMP (12 mM), ^{1}H and ^{31}P NMR pH titrations were performed at 298 K within the first 6 h, to record ^{1}H and ^{31}P NMR resonances for the intermediates Ru-*O*(PO_3)GMP and Ru-*O*(PO_3)GMP*N7*−Ru (Scheme 1).

For the reaction of $[(\eta^6\text{-Bip})\text{Ru(en)Cl}]^+$ (8 mM) with cGMP (9 mM), the mixture was incubated at 298 K for 24 h. This sample was then used directly for recording ^{1}H and ^{31}P NMR spectra at various pH values.

For the reaction of $[(\eta^6\text{-Bip})\text{Ru(en)Cl}]^+$ (12 mM) with 5′-IMP (14 mM), the mixture was incubated at 298 K for 24 h, followed by addition of a 14% molar excess of Ru. This mixture was used for a pH titration, which was completed within a further 4 h. The resultant ^{1}H and ^{31}P NMR spectra were recorded. The H8 and H2 chemical shifts of all six IMP species were subsequently plotted as a function of pH.

For the reaction of $[(\eta^6\text{-Bip})\text{Ru(en)Cl}]^+$ (5 mM) with inosine (6 mM), the mixture was incubated at 298 K for 12 h. ^{1}H NMR spectra were then recorded at various pH values.

For reactions of $[(\eta^6\text{-Bip})\text{Ru(en)Cl}]^+$ (10 mM) with 5′-CMP, 5′-TMP, or thymidine (10 mM), the mixtures were incubated at 310 K for 48 h, and ^{1}H and ^{31}P NMR spectra were then recorded at various pH values.

For reactions of $[(\eta^6\text{-Bip})\text{Ru(en)Cl}]^+$ with 5′-AMP, 10 parallel experiments were performed in ten NMR tubes under the similar conditions with various pH values over the range of 3−10. For each sample, the mixture of $[(\eta^6\text{-Bip})\text{Ru(en)Cl}]^+$ and 5′-AMP (1:1, 5 mM) with an adjusted pH was incubated at 310 K for 24 h, after which the pH value was determined again and used as the equilibrium pH value. Subsequently, ^{1}H and ^{31}P NMR spectra were recorded. The amount of phosphate-bound adduct at each of the 10 equilibrium pH values was determined by integration of either ^{1}H or ^{31}P NMR peaks.

Competitive Reactions of 5′-GMP, 5′-AMP, 5′-CMP, and 5′-TMP with $[(\eta^6\text{-Bip})\text{Ru(en)Cl}]^+$. 5′-GMP was mixed with one of three other nucleotides in a 1:1 mol ratio (5 mM, GMP + AMP, GMP + CMP, or GMP + TMP). Each of the combinations was then added to an aqueous solution of $[(\eta^6\text{-Bip})\text{Ru(en)Cl}]^+$ (final concentration 5 mM). The reaction mixtures were monitored immediately by ^{1}H and ^{31}P NMR spectroscopy at 298 or 310 K. The amounts of free and Ru-bound nucleotides were determined by peak integration.

Kinetic Studies. The reactions between chloro or aqua Ru(arene) complexes and nucleotides (5′-GMP, cGMP, 5′-IMP, 5′-AMP, cAMP, 5′-CMP, or 5′-TMP), or nucleosides (guanosine, inosine, adenine, cytosine, or thymidine), were carried out at a concentration of 5 mM Ru and 5 mM nucleobase in 10% D_2O/90% H_2O in NMR tubes. Most solutions were unbuffered to avoid interaction of buffer components with Ru(II). The solution pH was determined at the commencement of the reaction and after the establishment of equilibrium. The kinetic studies of various chloro or aqua Ru(arene) complexes with cGMP were carried out in 100 mM $NaClO_4$ at 298 K, pH 7.0. Due to the limited aqueous solubility of chloro Ru(THA) and Ru(DHA), the kinetics of reactions of various chloro Ru(arene) complexes with cGMP were performed at a concentration of 2 mM for both reactants. ^{1}H, ^{31}P NMR, or ^{15}N NMR data were recorded at appropriate time intervals. The first spectrum was acquired 10−15 min after mixing of the reactants, to allow time for temperature equilibration of the sample in the probe. Quantitation of the reactions was achieved by integration of the peaks for the base protons H8 (G), H8 and H2 (I and A), H6/H5 (C), and C(5)H_3 (T), or by integration of ^{31}P NMR peaks, or [^{1}H, ^{15}N] cross-peaks.

Methods and Instruments. NMR Spectroscopy. ^{1}H NMR spectra were acquired on a Bruker DMX 500 (^{1}H = 500 MHz) NMR spectrometer using TBI [^{1}H, ^{13}C, X] or triple resonance [^{1}H, ^{13}C, ^{15}N] probe-heads, respectively, and equipped with z-field gradients.

1D ^{1}H NMR spectra were typically acquired with 64 transients into 32 K data points over a spectral width of 6.0 kHz. Water suppression was achieved by presaturation. ^{31}P NMR spectra were obtained on a Bruker DMX 500 (^{31}P = 202 MHz) NMR spectrometer at 298 K, using inverse-gated ^{1}H decoupling. Typically 1D ^{31}P-{^{1}H} NMR spectra were acquired with 512 transients into 42 K data points over a spectral width of 40.7 kHz (200.8 ppm) using a relaxation delay of 1.3 s. Both 1D ^{15}N-edited ^{1}H NMR spectra and 2D [^{1}H, ^{15}N] HSQC NMR spectra (optimized for $^1J_{(NH)}$ = 73 Hz) were acquired using the sequence of Stonehouse et al.[15] A GARP decoupling sequence was used for ^{15}N decoupling during acquisition. Typically 1D ^{1}H-{^{15}N} NMR data were acquired with 16 transients into 1024 data points over a spectral width of 2.5 kHz (5.0 ppm) with a relaxation delay of 2.0 s. 2D [^{1}H, ^{15}N] HSQC NMR data were acquired with 4 transients into 1024 data points over a ^{1}H (F2) spectral width of 2.5 kHz (5 ppm, centered at the water resonance) for each of 256 t_1 increments (TPPI), and over a ^{15}N (F1) spectral width of 0.76 kHz (15 ppm, centered at −28 ppm) using a relaxation delay of 1.4 s between transients. Typically, 1D ^{1}H-{^{15}N} NMR spectra were acquired over a 10 min period and 2D [^{1}H, ^{15}N] HSQC NMR spectra were acquired over a 30 min period.

All data processing was carried out using XWIN NMR version 2.0 (Bruker U.K. Ltd.). ^{1}H NMR chemical shifts were internally referenced

(14) The purity of the aqua Ru(arene) complexes was confirmed by ^{1}H NMR. X-ray structures of the aqua adducts have been determined and will be reported elsewhere.

(15) Stonehouse, J.; Shaw, G. L.; Keller, J.; Laue, E. D. *J. Magn. Reson. Ser. A*, **1994**, *107*, 178−184.

to 1,4-dioxane (3.77 ppm) or to the methyl singlet of TSP (0 ppm) in aqueous solutions. ^{31}P resonances were referenced to 85% H_3PO_4 (external) at 0 ppm, and ^{15}N resonances to 1 M $^{15}NH_4Cl$ in 1.5 M HCl (external) at 0 ppm.

pH Measurements. The pH values of NMR samples in 10% D_2O/90% H_2O were measured at 298 K directly in the NMR tube, before and after recording NMR spectra, using a Corning 240 pH meter equipped with an Aldrich micro combination electrode calibrated with Aldrich buffer solutions at pH 4, 7, and 10. The pH values were adjusted with dilute $HClO_4$ and NaOH. No correction has been applied for the effect of deuterium on the glass electrode.

Calculation of pK_a Values. The pH titration curves were fitted to the Henderson−Hasselbalch equation using the program KALEIDAGRAGH,[16] with the assumption that the observed chemical shifts are weighted averages according to the populations of the protonated and deprotonated species.

Determination of Rate Constants. The reactions of aqua Ru(arene) complexes with cGMP (1:1, 5 mM) (Ru−H_2O + cGMP → Ru-*N7*cGMP) were analyzed as second-order processes (see Figure S8). The second-order rate constants (k) were determined by fitting kinetic curves of concentration versus reaction time for formation Ru-*N7*cGMP using the appropriate equation and the program Scientist (see Figure S9).

Results

To investigate the specificity of the binding of {(η^6-arene)-Ru(en)}$^{2+}$ to nucleobases, we have studied reactions of the anticancer complex [(η^6-Bip)Ru(en)Cl]$^+$ with various nucleosides and nucleotides (see Chart 1) in aqueous solution by ^{1}H, ^{15}N, and ^{31}P NMR spectroscopy. The binding sites for {(η^6-Bip)Ru(en)}$^{2+}$ on nucleobase derivatives were identified by ^{1}H NMR and ^{31}P NMR pH titrations, and each adduct was characterized by pK_a values derived from the pH titration curves. Some competition experiments were also performed to study the relative binding preferences of {(η^6-Bip)Ru(en)}$^{2+}$ toward mononucleotides. We have also investigated the influence of pH, chloride, and phosphate on the rate of binding of {(η^6-arene)Ru(en)X}$^{n+}$ (arene = Bip, THA, DHA, Cym, or Ben, and X = Cl or H_2O) complexes to 5′-GMP and cGMP by ^{1}H and ^{31}P NMR. The detailed kinetics for the reactions with cGMP were analyzed.

Reactions of [(η^6-Bip)Ru(en)Cl]$^+$ with Nucleotides and Nucleosides. Guanine Forms only N7 Adducts. Phosphate-bound Intermediates Detected for 5′-GMP but not for cGMP. The H8 region of the NMR spectrum of 5′-GMP after reaction with [(η^6-Bip)Ru(en)Cl]$^+$ (1:1, 5 mM, pH 7.15, 298 K) for 0.25−22 h is shown in Figure 1A. Three new H8 signals were observed: peak b (δ 8.027) appeared rapidly (during the reaction mixing time) and was shifted to low frequency relative to free 5′-GMP (peak a, δ 8.175), but disappeared at later times; peak d at higher frequency (δ 8.453) was evident after 2 h and finally disappeared as well; peak c appeared at higher frequency (δ 8.733), increased in intensity with time, and was the only final product observed for this reaction. An identical reaction, which was followed by ^{31}P NMR (Figure 1B), revealed corresponding changes in intensities of ^{31}P NMR peaks (a−d) which were consistent with the ^{1}H NMR results. However, for ^{31}P, there were large shifts in peaks b (δ 9.017) and d (δ 9.237) to high frequency relative to the resonance for free 5′-GMP (peak a, δ 3.899), compared with the slight high-frequency shift of peak c (δ 4.482). The reactions were complete within ca. 22 h.

(16) KALEIDAGRAPH, version 3.09; Synergy Software: Reading, PA, 1997.

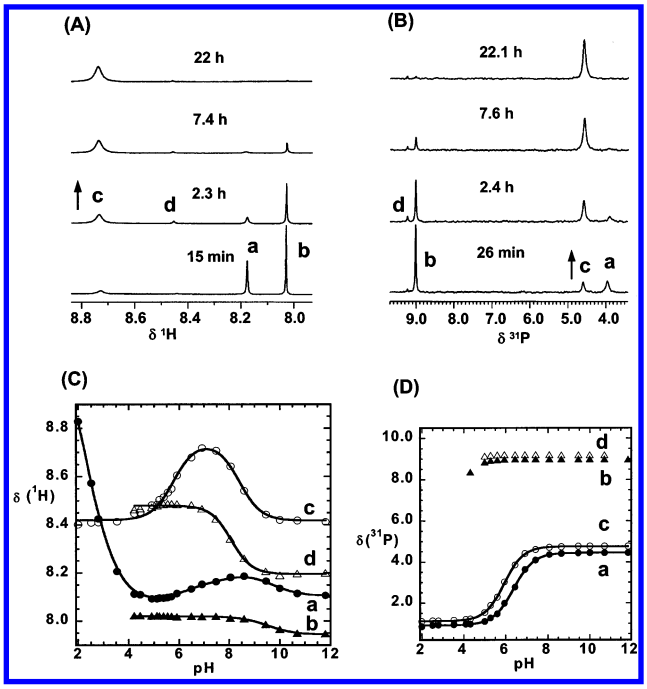

Figure 1. (A) ^{1}H, and (B) ^{31}P NMR spectra for the reaction of [(η^6-Bip)-Ru(en)Cl]$^+$ with 5′-GMP (1:1, 5 mM, pH 7.15, 298 K) at various reaction times. Plots of (C) H8 ^{1}H NMR chemical shift, and (D) ^{31}P NMR chemical shift vs pH for 5′-GMP species a−d. The curves are computer-fitted with the pK_a values listed in Table 1. The pH titration was performed for a similar reaction of [(η^6-Bip)Ru(en)Cl]$^+$ (12 mM) with 5′-GMP (12 mM). Peak assignments: a, free 5′-GMP; b, Ru−*O*(PO_3)GMP; c, Ru−*N7*GMP and d, Ru−*O*(PO_3)GMP*N7*−Ru. See Scheme 1 for structures.

Table 1. Selected Chemical Shifts and pK_a Values for 5′-GMP and cGMP and Their {(η^6-Bip)Ru(en)}$^{2+}$ Adducts at 298 K

species[a] (peak)[b]	pK_a (group)	δ (H8)[c]	δ (^{31}P)[c]
5′-GMP (a)	9.81 ± 0.10 (N1H)	8.175	3.899
	6.49 ± 0.18 (−PO_3H)		
	2.57 ± 0.01 (N7)		
Ru−*O*(PO_3)GMP (b)	9.51 ± 0.05 (N1H)	8.027	9.017
Ru−*N7*GMP (c)	8.39 ± 0.06 (N1H)	8.733	4.582
	5.77 ± 0.04 (−PO_3H)		
Ru−*O*(PO_3)GMP*N7*−Ru (d)	8.07 ± 0.04 (N1H)	8.453	9.237
cGMP (a)	9.67 ± 0.24 (N1H)	7.884	−0.979
	2.08 ± 0.02 (N7)		
Ru−*N7*cGMP (b)	8.13 ± 0.03 (N1H)	8.221	−1.022

[a] For structures see Schemes 1 and 2. [b] For peak labels see Figures 1 and 2. [c] For 5′-GMP, pH 7.20 and for cGMP, pH 7.28.

To identify the intermediates and products, a pH titration on a similar solution containing 12 mM Ru and 12 mM 5′-GMP was carried out during the first 6 h of reaction. Peaks b and d disappeared at pH values < 4, but the other peaks could be followed over the pH range 2−12. The ^{1}H and ^{31}P NMR titration curves are shown in Figure 1C and 1D, and associated pK_a values were determined by computer fits to the Henderson−Hasselbalch equation. The characteristic pK_a values associated with peaks a, b, c, and d, allow the intermediates to be assigned as Ru−*O*(PO_3)GMP (b), Ru−*O*(PO_3)GMP*N7*−Ru (d), and final product as Ru-*N7*GMP (c) (for structures see Scheme 1). Their pK_a values are listed in Table 1. Three pK_a values were determined for free 5′-GMP: 9.81, 6.49, and 2.57, attributable to the deprotonation of N1H, PO_3H, and N7, respectively. Ru−*O*(PO_3)GMP (peak b) undergoes deprotonation of N1H (pK_a of 9.51), but no deprotonation of PO_3H. Ru-*N7*GMP (peak c) undergoes deprotonation of PO_3H (pK_a of 5.77) and N1H (pK_a

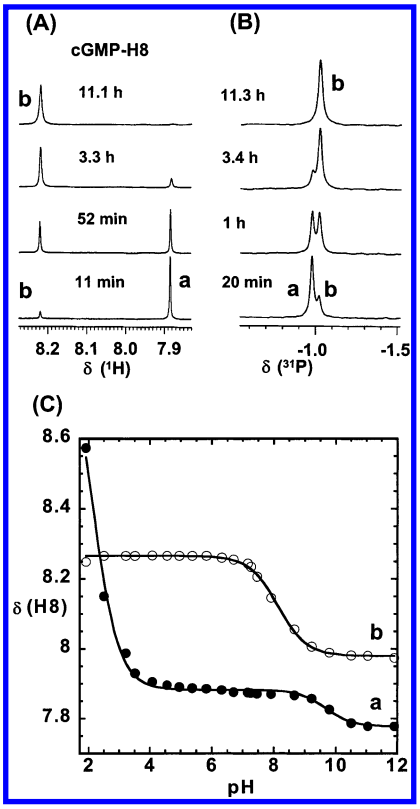

Figure 2. (A) ^{1}H, and (B) ^{31}P NMR spectra for the reaction of [(η^6-Bip)Ru(en)Cl]$^+$ with cGMP (1:1, 5 mM, pH 7.28, 298 K) at various reaction times. Peak assignments: a, free cGMP; b, Ru−*N7*cGMP. See Scheme 2 for structures. (C) Plots of H8 ^{1}H NMR chemical shifts of cGMP species a and b vs pH for a similar reaction with 8 mM Ru and 9 mM cGMP. The curves are computer best fits giving the pK_a values listed in Table 1.

of 8.39), but no deprotonation of N7. Ru−*O*(PO_3)GMP*N7*−Ru (peak d) undergoes deprotonation of N1H, but no deprotonation of PO_3H and N7. Notable is the lowering of the pK_a(N1) value by 1.42 units for Ru-*N7*GMP (peak c) and by 1.74 units for Ru−*O*(PO_3)GMP*N7*−Ru (peak d) compared to free GMP (peak a).

A similar reaction with 5′-GMP was also monitored by 2D [^{1}H, ^{15}N] HSQC NMR by use of ^{15}N-labeled [(η^6-Bip)Ru(en)Cl]$^+$ (Figure S1). Four species labeled Ru−Cl, Ru−H_2O, Ru−*O*(PO_3)GMP, and Ru−*N7*GMP were detected during the time course of the reaction (Figures S1 and S2). This result, together with the ^{1}H and ^{31}P NMR time courses, allowed reaction pathways to be drawn up, as shown in Scheme 1. First, the chloro complex Ru−Cl undergoes hydrolysis in water to give the reactive aqua complex Ru−H_2O, followed by rapid reaction with the 5′-phosphate of 5′-GMP, and then a slow displacement of bound phosphate by N7. The species distribution determined after 55 min of reaction is shown in Scheme 1.

The reaction of 3′, 5′-cyclic GMP (cGMP) with [(η^6-Bip)Ru(en)Cl]$^+$ (1:1, 5 mM, pH 7.28, 298 K) was monitored by ^{1}H and ^{31}P NMR for a period of ca. 12 h. After 11 min, a new H8 ^{1}H NMR peak (b, δ 8.221) was observed, shifted to high frequency by 0.337 ppm compared to free cGMP (peak a, δ 7.884), Figure 2A. This was the only new H8 signal observed, and after 12 h was the only H8 peak in the spectrum. In the ^{31}P spectrum (Figure 2B), only one new peak appeared (b, δ −1.022). This peak was shifted to low frequency by only 0.043 ppm relative to that for cGMP (peak a, δ −0.979). A pH titration of a similar reaction solution gave pK_a values of 9.67 and 2.08

Scheme 2. Scheme for Reaction of [(η^6-Bip)Ru(en)Cl]$^+$ with cGMP in Aqueous Solution at pH = 7.28, 298 K

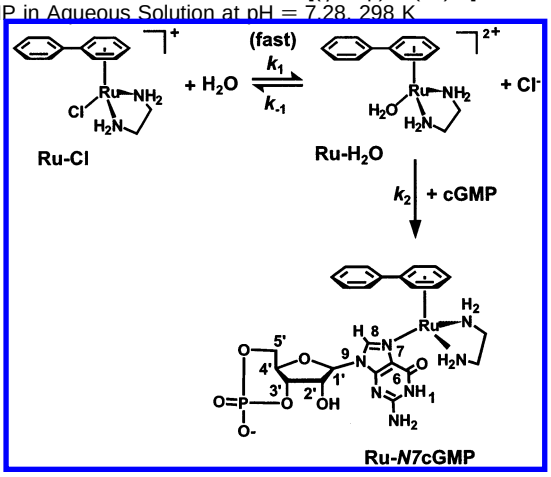

for peak a (free cGMP), and a single pK_a value of 8.13 for the product peak b, as derived from the H8 ^{1}H curves (Figure 2C and Table 1). Peak b can be assigned as Ru−*N7*cGMP (see Scheme 2). pK_a values of 9.67 (peak a) and 8.13 (peak b) are attributable to deprotonation of N1H. The pK_a value of 2.08 (peak a) is attributable to protonation of N7. Notable is the lowering of the pK_a for N1 by 1.54 units relative to free cGMP (peak b). During the reaction, no phosphate-bound adducts were detected. The reaction course is shown in Scheme 2. After 10 h, >95% of the cGMP was present as Ru−*N7*cGMP.

The reaction of guanosine (Guo) with [(η^6-Bip)Ru(en)Cl]$^+$ (1:1, 5 mM, 310 K, pH 7.20) was followed by ^{1}H NMR for 1 d. Only one new peak assignable[12] to Ru−*N7*Guo appeared at high frequency (δ 8.22) relative to free Guo (δ 7.9), and after 14 h, > 97% of Guo was present as Ru−*N7*Guo. A similar reaction was performed at pH 9.29, and only the Ru−*N7*Guo adduct was present after 14 h (Table S1).

Ru(II) Binds to N7 and N1 of Inosine, and Phosphate-Bound Intermediates are Formed with 5′-IMP. The reaction between 5′-IMP and [(η^6-Bip)Ru(en)Cl]$^+$ (1:1, 5 mM, pH 7.26) was monitored by ^{1}H and ^{31}P NMR spectroscopy. During the reaction, the pH value dropped from 7.26 (when mixed) to 6.55 (after 3 d at 310 K). The H8 and H2 regions of the ^{1}H NMR spectra of 5′-IMP at different reaction times are shown in Figures 3A-C. ^{31}P NMR peak assignments are given in Table 2. During the course of the reaction, 5 new sets of H8 and H2 peaks (peaks b, c, d, e, and f) were seen. Of these, 3 sets (peaks c, d, and e) are due to intermediates: their intensities decreased at later reaction times and almost disappeared after 3 d at 310 K. The intermediates and products were identified by a ^{1}H NMR pH titration on a similar solution (Figure 3D). It can be seen that peaks c, d, and e disappeared at lower pH (<5.8). From ^{1}H H8 shifts, the pK_a values associated with all 6 sets of IMP peaks were determined and are listed in Table 2. For free 5′-IMP (a), pK_a values of 9.22, 6.36, and 1.35 were determined for N1H, PO_3H, and N7, respectively, whereas peak b has two associated pK_a values of 7.74 and 5.71 assignable to N1H and PO_3H, but no pK_a assignable to N7. Peak b can therefore be assigned as Ru−*N7*IMP. Peak c has an N1H pK_a value of 9.04 and no associated phosphate pK_a, and is assigned to Ru−*O*(PO_3)IMP. Peak d has a PO_3H pK_a of 6.35 but no N1H pK_a, and is assigned to Ru−*N1*IMP. Peak e has no measurable pK_a values at all and is assignable to Ru−*O*(PO_3)IMP*N1*−Ru. Peak f has a PO_3H

Table 2. Selected Chemical Shifts and pK_a Values for 5′-IMP and Inosine (Ino) and Their {(η^6-Bip)Ru(en)}$^{2+}$ Adducts at 298 K

species[a] (peak)[b]	pK_a (group)[c]	δ (H8)[d]	δ (H2)[d]
5′-IMP (a)	9.22 ± 0.05 (N1H)	8.497	8.169
	6.36 ± 0.05 (PO_3H)		
	1.35 ± 0.01 (N7)		
Ru−*N7*IMP (b)	7.74 ± 0.03 (N1H)	9.053	8.131
	5.71 ± 0.03 (PO_3H)		
Ru−*O*(PO_3)IMP (c)	9.04 ± 0.03 (N1H)	8.404	7.909
Ru−*N1*IMP (d)	6.35 ± 0.05 (PO_3H)	8.339	8.016
Ru−*O*(PO_3)IMP*N1*−Ru (e)		8.330	7.99
Ru−*N7*IMP*N1*−Ru (f)	5.73 ± 0.03 (PO_3H)	8.856	8.155
Ino (a)	8.79 ± 0.02 (N1H)	8.344	8.225
	0.909 ± 0.003 (N7)		
Ru−*N7*Ino (b)	7.11 ± 0.04 (N1H)	8.745	8.201
Ru−*N1*Ino (c)		8.135	7.977
Ru−*N7*Ino *N1*−Ru (e)		8.624	8.165

[a] For structures, see Schemes 3 and 4. [b] For peak labels, see Figures 3 and 5. [c] On the basis of H8 chemical shifts. [d] pH 6.31 for 5′-IMP and pH 6.19 for Ino. For 5′-IMP, the corresponding ^{31}P NMR resonances appeared at δ 3.278 for peak a, δ 8.983 for c, and δ 8.272 for e, δ 3.410, 4.393, and 1.612 for peaks b, d, and f, but specific assignments were not made.

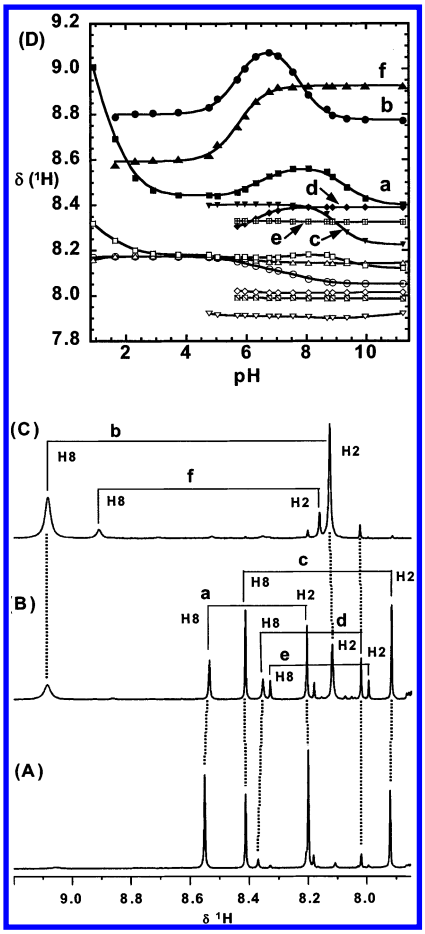

Figure 3. H8 and H2 region of ^{1}H NMR spectra for the reaction of 5′-IMP with [(η^6-Bip)Ru(en)Cl]$^+$ (1:1, 5 mM, initial pH 7.26) at 298 K after (A) 13 min (pH 7.15), (B) 3.7 h (pH 6.74), and (C) after a further 3 d at 310 K (pH 6.55). (D) Plots showing the variation with pH of H8 (solid symbols) and H2 (open symbols) ^{1}H NMR chemical shifts for species a−f.. pK_a values were determined from H8 shifts. Assignments: a, H8 (■) and H2 (□), free 5′-IMP; b, H8 (●) and H2 (○), Ru−*N7*IMP; c, H8 (▼) and H2 (▽), Ru−*O*(PO_3)IMP; d, H8 (◆) and H2 (◊), Ru−*N1*IMP; e, H8 (✸) and H2 (⊠), Ru−*O*(PO_3)IMP*N1*−Ru; and f, H8 (▲) and H2 (△), Ru−*N7*IMP*N1*−Ru. For structures see Scheme 3. Note that d, e, and f are N1-bound species.

pK_a of 5.73, but no N7 and N1 pK_a values and is assigned to Ru−*N7*IMP*N1*−Ru. The distribution of 5′-IMP species at pH

Scheme 3. Scheme for Reaction of [(η^6-Bip)Ru(en)Cl]$^+$ with 5′-IMP (1:1, 5 mM) in Aqueous Solution at pH = 7.28, 298 K. Species Distribution (%) is Shown after 24 h Reaction at 310 K, Based on H8 and H2 Intensities

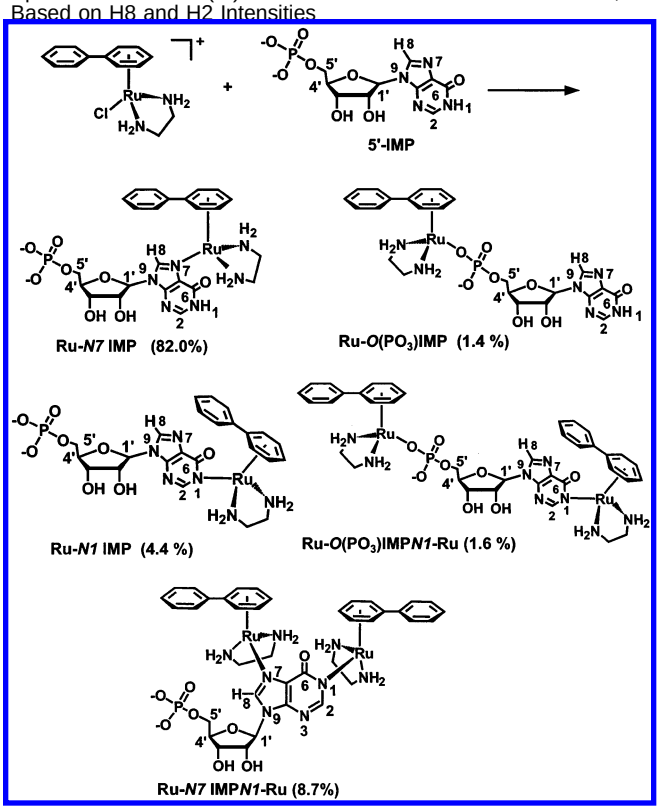

6.46 after 24 h at 310 K was determined by H8 and H2 peak integration and is shown in Scheme 3.

The reaction of inosine (Ino, 5.5 mM) with [(η^6-Bip)Ru(en)-Cl]$^+$ (5 mM) was followed by ^{1}H NMR for 2 d at 310 K with an initial pH of 7.22. After 1 d, the pH value of the solution had decreased to 6.19. A representative ^{1}H NMR spectrum for the H8 and H2 region is shown in Figure 4A. Three products are formed corresponding to 3 new sets of H8 and H2 peaks: b, d and c. The products were identified by ^{1}H NMR pH titration (Figure 4B, note that product c disappeared at pH < 4.0). The pK_a values are derived from H8 chemical shifts[17] and are listed in Table 2. Peak a has two associated pK_a values of 8.79 and 0.91, attributable to protonation of N1H and N7 of free inosine. Peak b has one pK_a value of 7.11, attributable to the protonation of N1H of Ru−*N7*Ino. After 24 h at 310 K, the species distribution was determined to be: Ru−*N7*Ino: 59.4%, Ru-*N1*Ino: 23.0%, Ru−*N7*Ino*N1*−Ru: 3.7% (Scheme 4). Species distributions and N(7)/N(1) binding ratios for reactions of Ino with [(η^6-Bip)Ru(en)Cl]$^+$ at various pH values (5.5−10.3) are listed in Table S1. With increase in pH, the N(7)/N(1) binding ratio decreased significantly from 7.72 (pH 5.5) to 0.22 (pH 10.3).

Little Reaction with cAMP or Adenosine, and Only 5′-Phosphate Binding for 5′-AMP. The reactions of 5′-AMP with [(η^6-Bip)Ru(en)Cl]$^+$ (1:1, 5 mM, 310 K) at various pH values were monitored for 24 h by ^{1}H and ^{31}P NMR spectroscopy (Figures S5A and S5B). A rapid reaction was observed (within

(17) Similar pK_a values were determined from H2 chemical shifts, e.g., pK_a values for N1H deprotonation were determined to be 8.78 for free Ino (a) and 7.14 for Ru−*N7*Ino (b), close to the values of 8.79 (a) and 7.11 (b) derived from H8 chemical shifts.

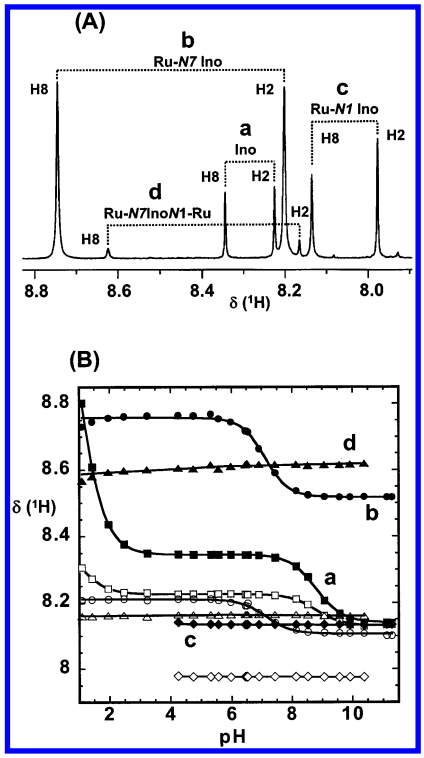

Figure 4. (A) The H8 and H2 region of the ^{1}H NMR spectrum of inosine (5.5 mM) after reaction with $[(\eta^6\text{-Bip})\text{Ru(en)Cl}]^+$ (5 mM) for 24 h at 310 K with initial pH 7.22. (B) Plots of H8 and H2 chemical shifts vs pH for the five species a−d detected during the above reaction. Peaks labels: H8, solid symbols; H2, open symbols, i.e., a, H8 (■) and H2 (□); b, H8 (●) and H2 (○); c, H8 (◆) and H2 (◇); d, H8 (▲) and H2 (△).

Scheme 4. Scheme for Reaction of $[(\eta^6\text{-Bip})\text{Ru(en)Cl}]^+$ (5 mM) with Inosine (5.5 mM) in Aqueous Solution at pH = 7.22. Species Distribution (%) is Shown after 24 h Reaction at 310 K, Based on H8 and H2 Intensities

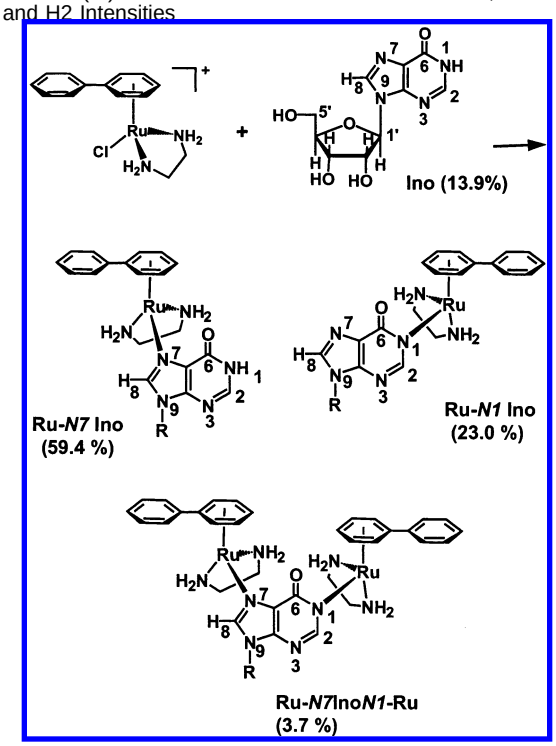

the time of mixing) which gave rise to one new set of H2 and H8 ^{1}H NMR signals (peak b, H2 δ 8.006 and H8 δ 8.402, pH 6.8), shifted to low frequency relative to free 5′-AMP (peak a, H2 δ 8.240 and H8 δ 8.555) and in slow exchange on the NMR time scale. Similarly, one new signal (peak b, δ 9.125) was observed in the ^{31}P NMR spectrum (Figure S5B) shifted to high frequency by 5.568 ppm (pH 6.8). The variation in intensity of ^{31}P NMR peak b with pH is shown in Figure S5C. It can been seen that it reached its maximum intensity at pH ca. 7.2 and decreased in intensity at either lower or higher pH; at pH 3.0, only free 5′-AMP peaks were seen, and at pH 9.6, > 90% of 5′-AMP was free. The variations of ^{1}H (H8 and H2) and ^{31}P NMR chemical shifts with pH are shown in Figure S7, and pK_a values determined from H8 ^{1}H NMR shifts are listed in Table 3. Free 5′-AMP (peak a) has two associated pK_a values of 6.41 and 4.05, attributable to the deprotonation of PO_3H and N1H, respectively. Peak b can be assigned to the phosphate-bound adduct Ru−*O*(PO_3)AMP and has no measurable pK_a value within the pH range 4−10.

Table 3. Selected Chemical Shifts and pK_a Values for 5′-AMP, 5′-CMP, 5′-TMP, Thymidine, and Their $\{(\eta^6\text{-Bip})\text{Ru(en)}\}^{2+}$ Adducts at 298 K

species (peak)[a]	pK_a [b](group)	δ (^{1}H)[c]	δ (^{31}P)
5′-AMP (a)	6.41 ± 0.07 (PO_3H) 4.05 ± 0.08 (N1H)	8.555	3.557
Ru−*O*(PO_3)AMP (b)		8.402	9.125
5′-CMP (a)	6.43 ± 0.04 (PO_3H) 4.36 ± 0.03 (N3H)	8.091	3.696
Ru−*O*(PO_3)CMP (b)		7.875	8.960
Ru−*N3*CMP (c)	6.12 ± 0.08 (PO_3H)	*d*	3.917
5′-TMP (a)	9.99 ± 0.03 (N3H) 6.65 ± 0.07 (PO_3H)	1.914	1.95
Ru−*N3*TMP (d)	6.32 ± 0.02 (PO_3H)	1.694	2.05
Ru−*O*(PO_3)TMP*N3*−Ru (b, c and e)		1.781, 1.754, 1.667	*e*
Thymidine (a)	9.76 ± 0.12 (N3H)	1.900	
Ru−*N3*Thymidine (b and c)		1.755, 1.677	

[a] For peak labels see Figures S5 and S6. [b] On the basis of H8 or H6 or T-CH_3 chemical shift. [c] H8 and pH 6.8 for 5′-AMP, H6 and pH 7.10 for 5′-CMP, CH_3 and pH 5.81 for 5′-TMP, and CH_3 and pH 5.37 for thymidine. [d] Peak c of H6 is overlapped with phenyl resonances in the ^{1}H NMR spectra. [e] ^{31}P NMR resonances at ca. δ 9.0 for Ru-*O*(PO_3) adducts, but specific assignments were not made for peaks b, c, and e due to overlap.

Reactions of cAMP and adenosine (Ado) with $[(\eta^6\text{-Bip})\text{Ru(en)Cl}]^+$ (1:1, 5 mM, 310 K) were monitored by ^{1}H NMR at different pH values (4.0, 7.0, and 9.0). Only small amounts (<5%) of products were formed for both cAMP and Ado, even after 3 d at 310 K (Table 4). These are possibly N7/N1 adducts (based on H8 and H2 chemical shifts). pH titrations were not attempted due to the low concentrations of products.

5′-CMP Forms 5′-Phosphate Adduct and a Minor N3 Adduct. Reactions of 5′-CMP with $[(\eta^6\text{-Bip})\text{Ru(en)Cl}]^+$ (1:1, 5 mM, pH 7.23, 310 K) were followed for up to 3 d, and ^{1}H and ^{31}P NMR spectra are shown in Figures S6A and B. A rapid reaction was observed and gave rise to a new H6 ^{1}H NMR peak shifted to low frequency (b, δ 7.875), which accounted for ca. 56% of the total 5′-CMP after 1 d. There was a corresponding new ^{31}P NMR peak (b, δ 8.960) shifted to high frequency by 5.264 ppm. In the ^{31}P NMR spectrum, an additional minor peak c appeared at 3.917 ppm. The corresponding H6 signal for peak c was not detected, perhaps due to peak overlap with the phenyl resonances. The ^{1}H and ^{31}P NMR pH titration curves are shown in Figure S7, parts C and D (note that peak b disappears at pH < 4.2). pK_a values were determined from H6 ^{1}H NMR shifts and are listed in Table 3. Free 5′-CMP (peak a) has pK_a values of 6.43 and 4.36, attributable to the deprotonation of PO_3H and N3H, respectively. Peak b can be assigned to Ru−*O*(PO_3)CMP,

Table 4. Reactions of Nucleosides and Nucleotides with $[(\eta^6\text{-Bip})\text{Ru(en)Cl}]^+$

nucleoside/nucleotide	species	% reaction[a] 1 d	% reaction[a] 3 d	pH 0	pH 1 d	pH 3 d
guanosine (Guo)	Ru−*N7*Guo	100	100	7.20	7.25	7.37
	Ru−*N1*Guo	0	0			
inosine (Ino)	Ru-*N7*Ino	59.4	54.3	7.22	6.19	5.9
	Ru-*N1*Ino	23.0	22.8			
	Ru-*N7*Ino*N1*−Ru	3.7	7.7			
thymidine	Ru-*N3*Thymidine	30.6	34.7	7.20	5.19	5.37
cytidine	Ru-*N3*Cytidine	11.6	13.5	7.24	7.19	7.33
adenosine (Ado)	Ru-*N7*/*N1* Ado	<3	<5	7.24	7.28	7.30
5′-GMP	Ru-*N7*GMP	>95	100[b]	7.10	7.22	7.26
	Ru-*O*(PO_3)GMP	< 5	0			
cGMP	Ru-*N7*cGMP	100		7.28	7.26	
5′-IMP	Ru-*N7*IMP	82.0	79.7	7.28	6.46	6.55
	Ru-*N1*IMP	4.4	3.1			
	Ru-*N7*IMP*N1*−Ru	8.7	12.5			
	Ru-*O*(PO_3)IMP*N1*−Ru	1.6	0.7			
	Ru-*O*(PO_3)IMP	1.4	0.5			
5′-TMP	Ru-*N3* adducts (b, c, d, e)	58.0	56.8 (2 d)	7.23	6.03	6.23 (2 d)
	Ru-*O*(PO_3) adducts (b, c and e)	46.8	47.2 (2 d)			
5′-CMP	Ru-*N3*CMP	8.6	7.4	7.23	7.10	7.10
	Ru-*O*(PO_3)CMP	56.1	40.7			
5′-AMP	Ru-*N7*/*N1* products	3.1	3.5 (2 d)	7.04	6.78	6.90 (2 d)
	Ru-*O*(PO_3)AMP	68.6	63.5 (2 d)			
cAMP	Ru−N7/N1 products	<5	<5	7.30	7.27	7.10

[a] On the basis of total nucleoside/nucleotide and determined by integration of ^{1}H or ^{31}P NMR resonances. Reaction conditions: Ru: nucleobase 5 mM: 5 mM (except for inosine: 5 mM: 5.5 mM), and at 310 K (298 K for cGMP). [b] To this sample NaCl (100 mM) was added and the solution was incubated at 310 K; reversal of 5′-GMP binding was very slow and amounted to only ca. 10% after 1 week.

and has no measurable pK_a value within the pH range 4−11. Peak c has an associated pK_a value of 6.12 (based on ^{31}P NMR titration), attributable to the deprotonation of PO_3H and can be assigned to the Ru−*N3*CMP product.

The reaction of cytidine with $[(\eta^6\text{-Bip})\text{Ru(en)Cl}]^+$ (1:1, 5 mM, pH 7.2) was monitored by ^{1}H NMR. On the basis of new biphenyl ^{1}H resonances, only 13% of cytidine reacted even after 3 d at 310 K (Table 4), possibly via N3 binding. A pH titration was not attempted due to the low concentration of the product.

Ru(II) binds to Phosphate and N3 of 5′-TMP. Reactions of 5′-TMP with $[(\eta^6\text{-Bip})\text{Ru(en)Cl}]^+$ (1:1, 5 mM, pH 7.2, 298 K) were followed by ^{1}H and ^{31}P NMR spectroscopy for up to 3 d. Due to the overlap of H5 and H6 and H1′ signals of TMP with those for biphenyl protons, the analysis for this reaction was based on the T-CH_3 signal. A rapid reaction was observed within 10 min and gave rise to one new T CH_3 peak c at δ 1.754 shifted to low frequency relative to that for free TMP (peak a, δ 1.914). After 2 h, peaks b (δ 1.781), d (δ 1.694), and e (δ 1.667) appeared and increased in intensity with time, with a decrease in intensity of peak c. The pH value of the solution decreased steadily during the reaction from 7.3 (initial) to 6.20 (1 d). The reaction reached equilibrium after 1.5 d, at which time the relative intensities of 5′-TMP CH_3 peaks were a, 39%; b, 24%; c, 15%; d, 12%; and e, 10%. A representative ^{1}H NMR spectrum of the T CH_3 region is shown in Figure S6C, and ^{1}H NMR pH titration curves are shown in Figure S7E. pK_a values were determined for peaks a and d (Table 3). Free 5′-TMP has pK_a values of 9.99 and 6.65 for N3H and PO_3H, respectively. Peak d shows one pK_a value of 6.32 for PO_3H, and the absence of deprotonation of N3H, and is assigned to Ru-*N3*TMP. Peaks b, c, and d all have no associated deprotonation for PO_3H and N3H and can be assigned to adducts of the type Ru−*O*(PO_3)TMP*N3*−Ru, possibly isomers.[18]

The reaction of $[(\eta^6\text{-Bip})\text{Ru(en)Cl}]^+$ with thymidine (1:1, 5 mM, pH 7.20) was monitored by ^{1}H NMR at 310 K. The pH of the solution decreased from 7.20 (initial) to 5.37 after 3 d, compatible with N3 coordination to Ru with concomitant N3H deprotonation. Two new thymidine CH_3 ^{1}H NMR peaks (b δ 1.755 and c δ 1.677) appeared at lower frequency compared to that for free thymidine (peak a, δ 1.90; Figure S6D). The pH titration curves for peaks a, b, and c are shown in Figure S7F, and pK_a values for free thymidine and its adducts are listed in Table 3. For free thymidine (peak a), the pK_a value of 9.76 is attributed to deprotonation of N3H. Peaks b and c both have no associated deprotonation of N3H and disappeared at pH < 3, and can therefore be assigned to two isomeric forms of Ru-*N3*Thymidine adducts.[19] After 3 d, N3-bound adducts accounted for 34.7% of the total thymidine. In contrast to the sharp doublet signal for the T CH_3 protons of free thymidine (peak a), signals b and c were broad, perhaps due to an exchange process.

Only 5′-GMP Forms Adducts with $[(\eta^6\text{-Bip})\text{Ru(en)Cl}]^+$ in Competition with 5′-AMP, 5′-CMP, or 5′-TMP. Reactions of $[(\eta^6\text{-Bip})\text{Ru(en)Cl}]^+$ with 5′-GMP in competition with either 5′-AMP, 5′-CMP or 5′-TMP in a 1:1 molar ratio (5 mM) at pH 7.2 were monitored by ^{1}H and ^{31}P NMR at 310 K. In each case, after 2 d, the only new peaks observed corresponded to those for Ru-*N7*GMP (data not shown).

Kinetics Studies. Phosphate, Chloride and Hydroxide Decrease the Rate of GMP N7−Binding. The kinetics of reactions of chloro and aqua Ru(Bip) with 5′-GMP and cGMP in various solutions (different NaCl and phosphate concentrations) and at various pH values were monitored by ^{1}H and ^{31}P NMR spectroscopy. The observed half-lives ($t_{1/2}$) for N7-binding are listed in Table 5. The kinetics of reaction of chloro Ru-(Bip) with Na_2HPO_4 (5 mM, 1:1, 298 K, initial pH 7.26) were also monitored by ^{1}H and ^{31}P NMR spectroscopy (Figure S4).

(18) (a) Renn, O.; Lippert, B.; Schollhorn, H.; Thewalt, U. *Inorg. Chim. Acta* **1990**, *167*, 123−130. (b) Pfab, R.; Jandik, P.; Lippert, B. *Inorg. Chim. Acta* **1982**, *66*, 193−204.

(19) At pH < 3, the competition for N3 binding by H^+ is strong and Ru−N3 complexation is not favoured at equilibrium.

Table 5. Half-Lives ($t_{1/2}$) for Formation of Ru−*N7* Bound Adducts of 5′-GMP and cGMP with $[(\eta^6\text{-Bip})Ru(II)(en)Cl]^+$ (Ru−Cl) and $[(\eta^6\text{-Bip})Ru(II)(en)(H_2O)]^{2+}$ (Ru−H_2O)

Ru–Cl/H_2O	G	conditions[a]	pH[b]	$t_{1/2}$ (h)[c]
Ru−Cl	5′-GMP	100 mM NaCl	7.25, 7.25	7.0
		5 mM phosphate	7.24, 7.30	5.0
		50 mM phosphate	7.22, 7.18	15.0
		H_2O	5.37, 5.41	1.1
			7.22, 7.26	3.1
			9.40, 9.13	5.0
Ru−H_2O	5′-GMP	H_2O	7.34, 7.59	1.8
			9.11, 9.40	4.0
Ru−Cl	cGMP	H_2O	7.30, 7.60	1.0
Ru−H_2O	cGMP	H_2O	5.60, 5.88	0.5
			7.16, 7.69	0.8
			9.22, 9.64	4.3

[a] Ru: G = 1:1, 5 mM, 298 K. [b] pH (start), pH (equilibrium). [c] $t_{1/2}$ from concentration versus time plots; rate constants were not determined.

The reaction reached equilibrium after 2 h, and the equilibrium constant (K) for formation of Ru-*O*(PO_3) was determined to be 3.2.

For the reactions of 5′-GMP with chloro Ru(Bip) in 100 mM NaCl, the $t_{1/2}$ value for formation of Ru-*N7*GMP was 7 h, with 89% of the 5′-GMP bound as Ru-*N7*GMP after two weeks. In 5 mM phosphate buffer, the $t_{1/2}$ was 5 h, with 95% of GMP bound as Ru-*N7*GMP after 4 d (Figure S3). In 50 mM phosphate buffer, the $t_{1/2}$ was more than 15 h, with only 50% Ru-*N7*GMP formed even after one week. Under similar conditions at pH ca. 7.3 in H_2O, the reaction of 5′-GMP with aqua Ru(Bip) was 1.7 times faster than that with chloro Ru(Bip), and the reaction of Ru(Bip) with cGMP was 3 times faster than with 5′-GMP. No phosphate binding was detected for cGMP reactions, see Figure 2 and Scheme 2. Therefore chloride, dianionic phosphate ions and 5′-phosphate groups compete with N7 for binding to Ru(II).

The reaction rate was also dependent on pH (Table 5). For the reactions with 5′-GMP, $t_{1/2}$ for formation of Ru-*N7*GMP increased from 1.1 to 5.0 h when the pH was raised from 5.37 to 9.40. Similarly for cGMP, the reactions were much faster at low pH. The $t_{1/2}$ for formation of Ru-*N7*cGMP increased from 0.5 to 4.3 h when the pH was increased from 5.60 to 9.22. Because the pK_a of H_2O in $[(\eta^6\text{-Bip})Ru(en)(H_2O)]^{2+}$ is 7.7, the hydroxo complex Ru−OH is the predominant species in solution at high pH,[20] and thus slows down Ru−N7 binding.

Arene-purine Hydrophobic Interactions Greatly Enhance N7-binding to GMP. Reactions of five Ru(arene) (arene = Bip, THA, DHA, Ben, and Cym) complexes with cGMP were investigated by ^1H and ^{31}P NMR under physiologically relevant conditions. Fitted plots of concentration vs time for the reaction of aqua Ru(arene) with cGMP (1:1, 5 mM, pH 7.0) are shown in Figure 6A, and the second-order rate constants (k)[21] are listed in Table 6. Reactions of cGMP with aqua Ru(THA), Ru(Bip) and Ru(DHA) complexes were more than 3 times faster (k = 14.7, 8.1, and 7.1 × 10^{-2} $M^{-1}\cdot s^{-1}$, respectively) than those for aqua Ru(Cym) and Ru(Ben) complexes (k = 2.5 and 1.1 × 10^{-2} $M^{-1}\cdot s^{-1}$, respectively). For the reactions of chloro Ru-(arene) complexes with cGMP (1:1, 2 mM), there were two steps: Ru−Cl hydrolysis followed by Ru−N7 binding (see Scheme 2). The observed $t_{1/2}$ values for formation of Ru−N7 adducts are listed in Table 6. No attempt was made to determine the rate constants. Plots of concentration against time are shown in Figure 6B. The sequence of $t_{1/2}$ values for the reactions of chloro Ru(arene) is consistent with that for analogous reactions of the aqua Ru(arene) complexes: Ru(THA) < Ru(Bip) < Ru-(DHA) ≪ Ru(Cym) < Ru(Ben) (Table 6). For the THA, Bip, and DHA complexes, 100% of the N7-bound product was observed after 2 d, whereas only ca. 80% of the N7-bound product formed for Cym and Ben complexes after 4 d.

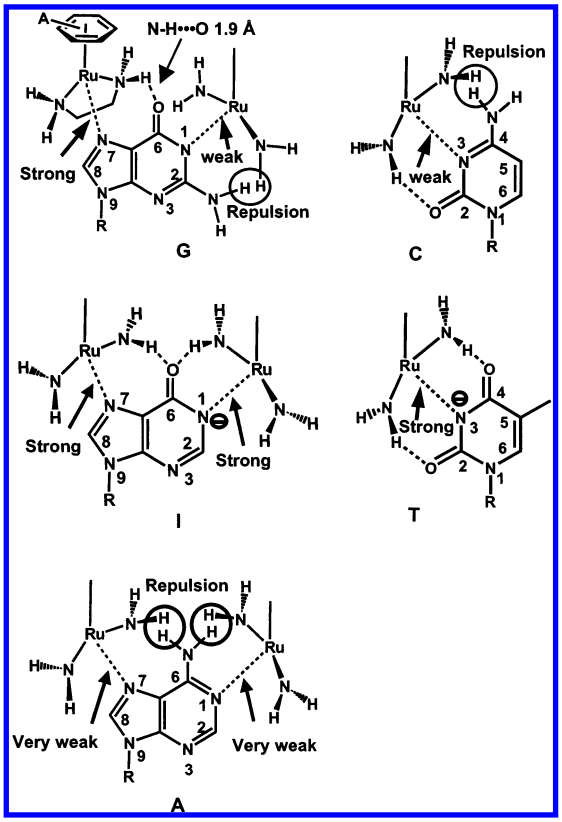

Figure 5. Regio- and stereo- specificities: H-bonds and nonbonding repulsions for the interaction of $\{(\eta^6\text{-arene})Ru(en)\}^{2+}$ with nucleobases, as detected in nucleoside and nucleotide reactions. For clarity, the arene and the CH_2CH_2 of the en ring have been omitted, except for the G adduct. For the purine adducts, the diagrams indicate in a general way the reactions with N7 and N1 and are not intended to apply specifically to the dinuclear adducts.

Discussion

Identification of Binding Sites. Purines exhibit a dichotomy between binding at N1 and N7. The proton favors N1. In neutral solution, N7 is usually the predominant binding site for transition metal ions on N9-substituted purines such as adenosine and guanosine. However, in adenine derivatives, N1 is only slightly less favorable than N7.[22] N1-substituted pyrimidines (cytidine, thymidine, uridine) offer only one favorable ring binding site, N3.[23] Reactions of purine and pyrimidine nucleosides and nucleotides with Pt(II) and Pd(II) complexes, for example, have been investigated previously, usually by ^1H and ^{31}P NMR

(20) Wang, F.; Chen, H.; Parsons, S.; Oswald, I.; Davidson, J.; Sadler, P. J., unpublished results.
(21) Half-lives were determined for the reactions of $[(\eta^6\text{-Bip})Ru(en)(H_2O)]^{2+}$ with cGMP at various initial concentrations under the same conditions (ratio 1:1, 298 K, pH 7.0 and 100 mM $NaClO_4$): 2 mM, $t_{1/2}$ = 105 min; 5 mM, $t_{1/2}$ = 41 min; 10 mM, $t_{1/2}$ = 17 min. These data confirm that the reaction is second order: $t_{1/2} = 1/C_A0\ k$ (k: $M^{-1}\cdot s^{-1}$, A = B).
(22) Martin, R. B.; Mariam, Y. H. *Metal Ions Biol. Syst.* **1979**, *8*, 57−124.
(23) (a) Lim, M. C.; Martin, R. B. *J. Inorg. Nucl. Chem.* **1976**, *38*, 1915−1918. (b) Schöllhorn, H.; Thewalt, U.; Lippert, B. *J. Am. Chem. Soc.* **1989**, *111*, 7213−7221.

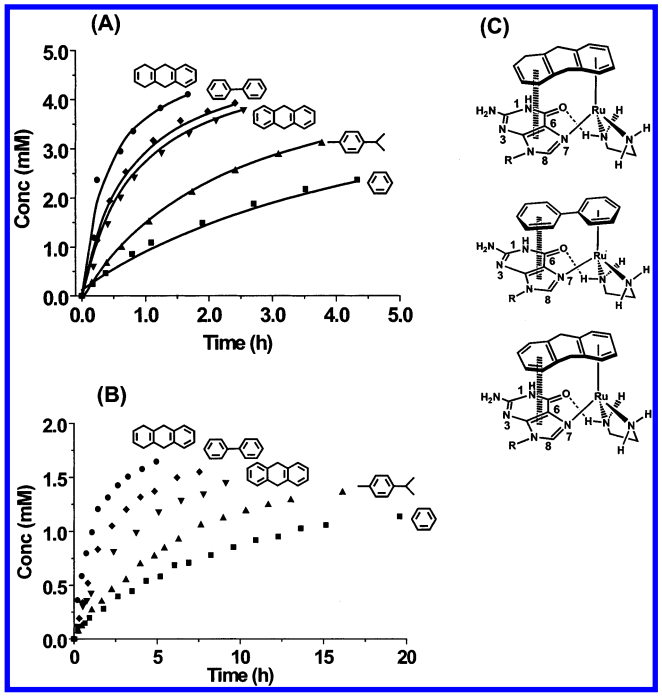

Figure 6. Plots showing the variation of the concentration of (η^6-arene)-Ru-*N7*cGMP products with time during the reaction of (A) [(η^6-arene)Ru-(en)(H_2O)]$^{2+}$ (5 mM), (B) [(η^6-arene)Ru(en)Cl]$^+$ (2 mM) with cGMP (1:1, pH 7.0), 100 mM $NaClO_4$, 298 K, based on the integration of G H8 ^{1}H NMR peaks. The curves in (A) are computer-fits to second-order kinetics giving the rate constants listed in Table 6. These reactions were all followed for periods of between 24 h and 4 days (see Figures S8 and S9). The reactions of the chloro complexes in (B) were followed for up to 1 week, and the half-lives for the formation of Ru−N7 adducts are shown in Table 6. No attempt was made to fit these data and determine the rate constants. (C) Posssible $\pi-\pi$ stacking between arene and purine in cGMP adducts with Ru(THA), Ru(Bip), and Ru(DHA).

Table 6. Rate Constants (k) and Half-lives ($t_{1/2}$) for Reactions of Ru(arene) Complexes with cGMP[a]

aqua Ru(arene)[b]	rate constant ($\times 10^{-2}$ $M^{-1}s^{-1}$)	$t_{1/2}$(h)[c]	chloro Ru(arene)[b]	$t_{1/2}$(h)[d]
Ru(THA)(H_2O)	14.72 ± 0.69	0.38 ±0.02	Ru(THA)Cl	1.1
Ru(Bip)(H_2O)	8.06 ± 0.15	0.69 ±0.01	Ru(Bip)Cl	2.0
Ru(DHA)(H_2O)	7.08 ± 0.20	0.78 ± 0.02	Ru(DTA)Cl	3.6
Ru(Cym)(H_2O)	2.49 ± 0.03	2.23 ± 0.03	Ru(Cym)Cl	7.1
Ru(Ben)(H_2O)	1.13 ± 0.02	4.94 ± 0.09	Ru(Ben)Cl	13

[a] Conditions: Ru: G = 1:1, 100 mM $NaClO_4$, 298 K, 5 mM for aqua Ru(arene) and 2 mM for chloro Ru(arene); pH was adjusted to 7.0 at reaction commencement and found to be ca. 7.2 at equilibrium for each reaction. [b] For the THA, Bip and DHA complexes, 100% of the N7-bound products observed after 2 d, whereas only ca. 80% of the N7-bound products formed for Cym and Ben complexes after 4 d. [c] Calculated from $t_{1/2} = 1/kC°$, $C° = 5.0$ mM. [d] $t_{1/2}$ from concentration versus time plots; rate constants were not determined.

spectroscopy.[24−26] Resolution of the N7−N1 dichotomy is unequivocal in the cases of Pt(II) and Pd(II) because the metal ion is both diamagnetic and, on the NMR time scale, in slow exchange between the two sites. Similarly, in this study, the diamagnetic nature of Ru(II), together with slow ligand exchange, allow the acid−base properties of the products to be individually assessed by pH titrations, and the populations of all species in solution can be determined through measurement of NMR peak areas. ^{31}P NMR was also used to reveal directly the interaction between Ru(II) and the phosphate group.[26c,27] Thus, we have been able to assess the selectivity of {(η^6-arene)-Ru(en)}$^{2+}$ complexes toward binding sites on purine and pyrimidine nucleic acid derivatives.

Adducts of {(η^6-arene)Ru(en)}$^{2+}$ with nucleosides and nucleotides exhibited characteristic ^{1}H and ^{31}P NMR signals, and acid−base properties which allow their structures to be assigned (Figures 1−4 and S6−7, and Tables 1−3). In the cases of 5′-GMP, cGMP, Guo, 5′-IMP, and Ino, metalation at N7 gave Ru−*N7* products with high-frequency shifts of 0.3−0.6 ppm for H8 resonances, but slight low-frequency shifts of 0.02−0.04 ppm for H2 resonances, compared with free ligands. Metalation at N1 (only found in the reactions with 5′-IMP and Ino) gave Ru−*N1* products with low-frequency shifts of 0.16−0.21 ppm for H8 and 0.22−0.26 ppm for H2 resonances. A similar chemical shift behavior for H8 and H2 protons upon metalation at N7 or N1 sites of purines has been reported for other metal ions.[25a] For all nucleotides, the ^{31}P NMR resonances exhibit large downfield shifts of ca. 5 ppm when the phosphate group coordinates to the Ru center (Tables 1−3).

The pH dependences of ^{1}H and ^{31}P NMR chemical shifts of nucleobase derivatives were studied in detail. Protonation of N7, N1, N3, or 5′-phosphate produced significant low- or high-frequency shifts of ^{1}H or ^{31}P NMR resonances (Figures 1-4 and S7). Ru(II) binding to N7, N1, N3, or the 5′-phosphate group prevents the protonation of that site, and therefore, no change in chemical shift due to protonation is expected. Therefore, the Ru(II) binding sites can be identified, as shown in Tables 1−3. It is notable that small amounts of dinuclear adducts[28] of the type Ru−*N7***B***N1*−Ru and Ru−*O*(PO_3)**B***N1*(*N7*)−Ru (**B** = nucleosides and nucleotides) were detected in solution. Binding site identification was supported by the following. (1) The significant pH decrease (from 7.2 to ca. 6) during reactions with I and T derivatives, is indicative of N1-coordination to Ru for 5′-IMP or inosine, and N3-coordination for 5′-TMP and thymidine, with concomitant deprotonation. This was not observed for reactions with G and A and C derivatives for which almost no N1 or N3-binding occurred (Table 4). (2) Ru−*N7* adducts have lowered pK_a values of 1.4−1.7 units for N1, and of 0.6−0.7 units for 5′-phosphate groups, but Ru−*O*(PO_3) binding causes only a small lowering of pK_a values of 0.18−0.30 for N1, and Ru−*N1* binding has little effect on the pK_a values of 5′-phosphate groups, relative to the free ligands (Tables

(24) (a) Martin, R. B. In *Cisplatin-Chemistry and Biochemistry of a Leading Anticancer Drug*; Lippert, B., Ed.; Wiley-VCH: Weinheim, Germany 1999; pp 183−205. (b) Martin, R. B. In *Platinum, Gold, and Other Metal Chemotherapeutic Agents: Chemistry and Biochemistry*; Lippard, S. J., Ed.; American Chemical Society, Washington, DC, 1983, ACS Symp. Ser. 209, pp 231−244.
(25) (a) Scheller, K. H.; Scheller-Krattiger, V.; Martin, R. B. E. *J. Am. Chem. Soc*. **1981**, *103*, 6833−6839. (b) Vestues, P. I.; Martin, R. B. *J. Am. Chem. Soc*. **1981**, *103*, 806−809. (c) Sovago, I.; Martin, R. B. *Inorg. Chem*. **1980**, *19*, 2868−2871.
(26) (a) Dijt, F. J.; Canters, G. W.; den Hartog, J. H. J.; Marcelis, A. T. M.; Reedijk, J. *J. Am. Chem. Soc.* **1984**, *106*, 3644−3647. (b) Miller, S. K.; Marzilli, L. G. *Inorg. Chem*. **1985**, *24*, 2421−2425. (c) Reily, M. D.; Hambley, T. W.; Marzilli, L. G. *J. Am. Chem. Soc*. **1988**, *110*, 2999−3007.
(27) (a) Alessio, E.; Xu, Y.; Cauci, S.; Mestroni, G.; Quadrifoglio, F.; Viglino, P.; Marzilli, L. G. *J. Am. Chem. Soc.* **1989**, *111*, 7068−7071. (b) Reily, M. D.; Marzilli, L. G. *J. Am. Chem. Soc.* **1986**, *108*, 8299−8300.
(28) Small amounts of the dinuclear species Ru−*N7*IMP*N1*−Ru (8.8%, pH 6.4) for 5′-IMP and Ru−*N7*Ino*N1*−Ru (3.7%, pH 6.24) for inosine, were detected at equilibrium. Both exhibited some stability at pH < 3 (Figures 4 and 5). Similar types of dinuclear M−*N7***B***N1*−M complexes have been detected previously in reactions of {dienPd}$^{2+}$ with all three purine 5′-nucleoside monophosphates GMP, IMP, and AMP at equilibrium: Pd−*N7*GMP*N1*−Pd (15%, pH 7.1), Pd−*N7*AMP*N1*−Pd (14%, pH 6.1), Pd−*N7*IMP−*N1*−Pd (14%, pH 6.4) and Pd-*N7*Ino*N1*−Pd (15%, pH 6.2), see ref 25 Metalation at N7 promotes the acidity of the proton at N1 by up to ca. 1.5 units, and therefore the binding of Ru to Ru−*N7***B**N1H can occur at the lower pH values compared to the free ligand **B**N1H.

1−3). These data are consistent with metalation at N7 which usually acidifies the proton at N1,[29−31] and consistent with the presence of an outer-sphere interaction involving H-bonding of the 5′-phosphate group to an en NH proton in Ru-*N7* adducts (but not in Ru−*N1* adducts) which can contribute to the larger lowering of the pK_a value of 5′-PO_3H for Ru−*N7* adducts compared to Ru−*N1* adducts.[25b,32,33] (3) Ru−*O*(PO_3), Ru−*N1* and Ru−*N3* adducts disappeared at pH < 5.0 (Figures 1, 3, 4 and S7), due to protonation of N1 and the 5′-phosphate group.[34]

Selective Recognition of Nucleobases. A summary of the extent of reaction of various nucleosides and nucleotides with $[(\eta^6\text{-Bip})\text{Ru(en)Cl}]^+$ is given in Table 4. Nucleotides and their corresponding nucleosides have similar affinities for Ru, except for a significant amount of 5′-phosphate binding in the former case. A schematic representation of the possible interactions between the nucleobases and the en NH_2 groups is given in Figure 5. H-bonding and nonbonding repulsive interactions, in addition to the electronic properties of the various nucleobase coordination sites,[35] appear to play key roles in these site-selective reactions.[3b] For G, N7 is the favored site for Ru(arene) binding. Our previous studies of Ru−N7 guanine adducts have revealed a strong H-bonding interaction between one en NH (pointing toward the G base) and G C6O with N···O distance 2.8 Å and N−H···O angle 163°, which is present in the X-ray crystal structures of $[(\eta^6\text{-Bip})\text{Ru(en)(9EtG)}]^{2+}$ and $[(\eta^6\text{-Bip})\text{Ru(en)(Guo)}]^{2+}$. Such high stereospecific H-bonding has also been detected in aqueous solution by NMR.[12] Thus, coordination at N7 is stabilized by H-bonding of en NH_2 with G C6O and coordination at N1 is unfavorable due to the repulsive interaction of en NH_2 with G2 NH_2. This is consistent with the data for reactions of Ru(Bip) with Guo, 5′-GMP and cGMP: only Ru−N7 adducts were detected (and no Ru−N1 adducts) over the pH range 2−12 (Tables 1 and S1). Inosine (I), in contrast to G, has no NH_2 group. Coordination at either N7 or N1 can be stabilized by H-bonding of en NH with C6O, and significant amounts of Ru−*N7* and Ru−*N1* adducts were detected for reactions of inosine and 5′-IMP with Ru(Bip) (Table 4). Binding at N1 is promoted at high pH with the concomitant deprotonation of N1H (Table S1). Adenine (A) has a C6 NH_2 group and coordination at either N7 or N1 of A is weakened by repulsive interactions with the exocylic amino group: no base-binding was observed for reactions of Ru(Bip) with Ado, cAMP or 5′-AMP over the range pH 3.1−9.6 (Table 4, Figure S5). For thymine (T), significant amounts of Ru−N3 adducts were formed in reactions of Ru(Bip) with both thymidine and 5′-TMP at pH ca. 6.0 (Table 4). Coordination at N3 may be favored by H-bonds between en NH and the exocyclic oxygens at C2 and C4,[36] For C, only small amounts of Ru−*N3* adducts (ca. 10%) were found for reactions of cytidine and 5′-CMP (Table 4). Coordination at N3 is weak due to the repulsive interaction of en NH with the C4 NH_2 group.

On the basis of the above nucleoside and nucleotide studies, the reactivity of the various binding sites of nucleobases[37] toward Ru(Bip) at neutral pH decreases in the order G(N7) > I(N7) > I(N1), T(N3) > C(N3) > A(N7), A(N1). In competitive binding experiments with 5′-GMP versus either 5′-AMP or 5′-CMP or 5′-TMP, the only final adduct was $[(\eta^6\text{-Bip})\text{Ru(II)(en)}(N7\text{-GMP})]$. Also in enzymatic digestion experiments, it was found that the binding of $[(\eta^6\text{-}p\text{-cymene})\text{Ru(en)Cl}]^+$ to a 14-mer oligonucleotide occurred specifically at guanine sites.[11] Experiments on the inhibition of RNA synthesis show that the termination sites produced by $\{(\eta^6\text{-arene})\text{Ru(en)}\}^{2+}$ adducts of DNA are at guanine residues.[38] Such a high specificity for guanine-N7 does not appear to have been reported for other metal-based anticancer agents. Many other Pt and Ru anticancer complexes also bind covalently to adenine. The complex $[\text{Ru(II)}(NH_3)_5\text{Cl}]^+$ reacts with many nitrogen bases,[31b] preferentially with the N7 of guanine,[31a] N1 of adenine[39] and N4 of cytosine.[31b] For *cis*-$[\text{Ru(II)}(\text{DMSO})_4\text{Cl}_2]$, the reaction sites in double-stranded polynucleotides are thought to be N7 of both guanine and adenine.[40] The trifunctional organometallic complex $[(\eta^6\text{-Ben})\text{Ru}(H_2O)_3]^{2+}$ binds to both N7 and N1 of adenine.[41] *Cis*-$\{(NH_3)_2\text{Pt(II)}\}^{2+}$ binds to adenosine at both N7 (55%) and N1 (45%),[42] and the monofunctional complex $\{(\text{dien})\text{Pt(II)}\}^+$ also binds to adenosine at both N7 (50%) and N1 (50%).[23a] *Cis*-$\{(NH_3)_2\text{Pt(II)}\}^{2+}$ forms both GG and AG intrastrand cross-links that account for about 65% and 25%, respectively, of DNA platinations.[43] Organometallic metallocene dichloride antitumor agents of the type $[Cp_2MCl_2]$ (M = Mo, Ti) exhibit little, if any, coordinative selectivity in nucleotide competition experiments.[44,45] The anti-HIV agent Zn(II)-[12]aneN_4 shows a high selectivity for N3 of thymine and uridine derivatives among all of the nucleobases, with formation of cyclen NH H-bonds to the C2 and C4 carbonyl oxygens of T or U.[46]

The ability of the NH proton of ethylenediamine to act as an H-bond donor toward an exocyclic oxo group but not toward an amino group appears to play an important role in controlling site recognition of the nucleobases by these Ru(arene) anticancer agents. When the en ligand is replaced by H-bond acceptor ligands (such as acetylacetonate derivatives), the Ru(arene) can also recognize adenine bases.[47] Initial data suggest that there is

(29) (a) Inagaki, K.; Kidani, Y.; *J. Inorg. Biochem*. **1979**, *11*, 39−47. (b) Schröder, G.; Lippert, B.; Sabat, M.; Lock, C. J. L.; Faggiani, R.; Song, B.; Sigel, H. *J. Chem. Soc., Dalton Trans*. **1995**, 3767−3775.

(30) Guo, Z.; Sadler, P. J.; Zang, E. *J. Chem. Soc., Chem. Commun.* **1997**, 27−28.

(31) (a) Clarke, M. J.; Taube, H. *J. Am. Chem. Soc*. **1974**, *96*, 5413−5419. (b) Clarke, M. J. *Met. Ions Biol. Syst*. **1980**, *11*, 231−283. pK_a(N1) is lowered by 0.8 for $[\text{Ru(II)}(NH_3)_5\text{(Guo)}]^{2+}$ (pK_a(N1) 8.7) and 2.2 for $[\text{Ru(III)}(NH_3)_5\text{(Guo)}]^{3+}$ (pK_a(N1) 7.36). The acidifying effect of Ru(II) is therefore less than that of Ru(III).

(32) Berners-Price, S. J.; Frey, U.; Ranford, J. D.; Sadler, P. J. *J. Am. Chem. Soc*. **1993**, *115*, 8649−8659.

(33) Reily, M. D.; Marzilli, L. G. *J. Am. Chem. Soc*. **1986**, *108*, 6785−6793.

(34) Small amounts of dinuclear Ru−*N7BN1*−Ru adducts (2%) still persist at pH < 3. There is enhanced stability of Ru−N1 binding via formation of dinuclear Ru−*N7BN1*−Ru adduct.

(35) Despite the similar acid−base properties of the nucleophilic sites of guanosine (G) and inosine (I) (see Tables 1 and 2, and ref 3b), $\{(\eta^6\text{-Bip})\text{Ru(en)}\}^{2+}$ coordinates to the N1 site of I but not of G. This suggests that interactions between the Ru en NH_2 groups and the exocyclic groups on the bases play a major role in controlling site selectivity.

(36) The pK_a(N3H) value of thymidine is 9.76 (Table 3). Protonation of N3 competes with Ru−N3 binding, and partially explains T did not fully react with Ru(Bip) at lower pH (7.2−5.8).

(37) In Watson−Crick double-helical DNA, N3 of thymine and cytosine would not be expected to be available for binding to Ru(II) because N3 is involved in H-bonding in base-pairs. N3 binding would therefore be restricted to regions of single-stranded DNA. Competitive experiments at pH 7.2 show that N3-binding to T or C is weak compared to G N7.

(38) Chen, H.; Nováková, O.; Zaludová, R.; Brabec, V.; Sadler, P. J., unpublished results.

(39) Clarke, M. J. *J. Am. Chem. Soc*. **1978**, *100*, 5068−5075.

(40) Cauci, S.; Alessio, E.; Mestroni, G. *Inorg. Chim. Acta* **1987**, *137*, 19−24.

(41) Korn, S.; Sheldrick, W. S. *J. Chem. Soc., Dalton Trans.* **1997**, 2191−2199.

(42) Arpalahti, J.; Lehikoinen, P. *Inorg. Chim. Acta* **1989**, *159*, 115−120.

(43) Fichtinger-Schepman, A.-M. J.; van der Veer, J. L.; den Hartog, J. H. J.; Lohman, P. H. M.; Reedijk, J. *Biochemistry* **1985**, *24*, 707−713.

(44) Kuo, L. Y.; Kanatzidis, M. G.; Sabat, M.; Tipton, A. L.; Marks, T. J. *J. Am. Chem. Soc*. **1991**, *113*, 9027−9045.

(45) Guo, M.; Guo, Z.; Sadler, P. J. *J. Biol. Inorg. Chem*. **2001**, *6*, 698−707.

(46) Shionoya, M.; Kimura, E.; Shiro, M. *J. Am. Chem. Soc*. **1993**, *115*, 6730−6737.

a correlation between the anticancer activity of Ru(arene) complexes and the presence of an en NH H-bond donor group. Activity is lost when the en NH_2 hydrogens are substituted, e.g., with methyl groups.[48] The choice of the specific chelating ligand appears to be an effective way of controlling selectivity for nucleobase recognition by octahedral Ru complexes. The steric constraints for nucleobase binding to an octahedral site are much more demanding compared to those for binding at a square-planar site, e.g., Pt(II).

Phosphate Binding. The first stage in reactions of $[(\eta^6\text{-Bip})\text{Ru(en)Cl}]^+$ with nucleotides (5′-GMP, 5′-IMP, 5′-AMP, 5′-CMP, and 5′-TMP) involved rapid 5′-phosphate binding (Figures 1 and 3, Table 4).[49] The phosphate adducts of 5′-GMP and 5′-IMP rearranged into N7 and N1 adducts, but for adenine, cytidine, and thymidine nucleotides, significant amounts of phosphate complexes were still present at equilibrium (Table 4). For 5′-AMP reactions, it can been seen that Ru−*O*(phosphate) binding is sensitive to pH, reaching a maximium at pH 7.2 (Figure S5). Lower pH values promoted protonation of the 5′-phosphate group, and higher pH values promoted the competitive binding of OH^- and thus reduced the formation of the 5′-phosphate adducts. Similarly, inorganic dianonic phosphate ions were also found to bind rapidly to $\{(\eta^6\text{-Bip})\text{Ru(en)}\}^{2+}$ to form a Ru−*O*(PO_3) product (Figure S4). Thus binding of $\{(\eta^6\text{-Bip})\text{Ru(en)}\}^{2+}$ to N7 of 5′-GMP was significantly retarded by phosphate buffers at neutral pH (Figure S3 and Table 5). In contrast, no binding of Ru(II) to the phosphodiester group of cGMP or cAMP was detected (Figure 2).

At neutral pH, *cis*-$[PtCl_2(NH_3)_2]$ forms monodentate adducts with the inorganic ortho-, pyro- and tri-phosphate ions,[50] and an N7, PO macrochelate *cis*-$[Pt(NH_3)_2$(5′-GMP-*N7, PO*)] with the nucleotide 5′-GMP, but does not bind to the phosphate group of the methyl phosphate diester of 5′-GMP (Me-5′-GMP).[51] $\{Cp_2Mo\}^{2+}$ coordinates to nucleotides (5′-dAMP, 5′-dCMP and 5′-dTMP) through Mo−*N7*/*N3* and Mo−*O*(phosphate) chelation, but does not show direct phosphate coordination to the methyl-phosphate diester of 5′-dGMP (Me-5′-dGMP)), diphenyl phosphate ($(C_6H_5O)_2P(O)OH$), or diethyl phosphate ($(CH_3CH_2O)_2P(O)OH$).[52] Zn(II) cyclen also acts as a good monotopic receptor for dianionic phosphate monoesters.[53] ^{1}H NMR studies of reactions of Zn(II)-bis(cyclen) with 5′-dTMP and 5′-dTDP indicate that the terminal phosphate dianion interacts with one of the Zn(II)-cyclens and the imido anion of dT binds to the other Zn(II)-cyclen.[54] Zinc-containing carboxylate-bridged heterodimetallic complexes can react with the phosphodiester ligand diphenyl phosphate to form bis(phosphate) complexes.[55] $\{(NH_3)_5\text{Ru(III)}\}^{3+}$ does not appear to coordinate directly to 5′-phosphate groups of nucleotides,[56] but the chelation of N7 and phosphate group of 5′-(d)GMP with *cis/trans*-[Ru(II)Cl_2(DMSO)],[57] and *N7,O(P)*-macrochelation of adenosine and guanosine 5′-mono-, -di-, and -tri-phosphates[41] with $[(\eta^6\text{-Ben})\text{Ru(II)}(H_2O)_3]^{2+}$ have both been detected by ^{1}H and ^{31}P NMR pH titrations. The latter organometallic complex is also capable of coordinating to the phospho- diester group of 5′-ADP.[41]

The $\{(\eta^6\text{-arene})\text{Ru(II)(en)}\}^{2+}$ complexes studied here bind to dianionic phosphate and phosphomonoesters, but very weakly to phosphodiesters. This has potential biological implications. The reversible binding to phosphate[58] as well as transient binding to membrane phospholipids may facilitate cellular uptake[59] of Ru(arene) species. Direct Ru(II) coordination with the backbone phosphodiester groups of DNA will be weak, but electrostatic interactions and H-bonding may be involved in the initial recognition of $[(\eta^6\text{-arene})\text{Ru(II)(en)}(H_2O)]^{2+}$ prior to binding to guanine N7, as proposed for some Pt complexes.[60]

Kinetic Studies. The rate of reaction of $[(\eta^6\text{-Bip})\text{Ru(en)X}]^{n+}$ with N7 of GMP depends on whether Cl^-, H_2O, OH^-, or phosphate occupies the available coordination position (X). Chloro Ru(arene) complexes rapidly hydrolyze in water to give more reactive aqua Ru(arene) species (Scheme 1 and Figures S1 and S2). Hydrolysis is suppressed in the presence of 100 mM chloride ions. The intracellular chloride concentration (ca. 4−23 mM) is significantly lower than the extracellular concentration (ca. 103 mM).[61] Thus, reactive Ru−H_2O species are likely to predominate inside cells under physiological conditions. The reactions of $[(\eta^6\text{-Bip})\text{Ru(en)}(H_2O)]^{2+}$ with both 5′-GMP and cGMP are more than 3 times slower at pH 9 compared to pH 5 to 7 (Table 5). This is attributable to the lower reactivity of Ru−OH compared to Ru−OH_2 (as is also the case for am(m)ino Pt(II) complexes), since the pK_a values for $[(\eta^6\text{-arene})\text{Ru(en)}(H_2O)]^{2+}$ complexes studied here are all within the range 7.7−8.25 (Figure S10).[20,62]

Arene-purine Hydrophobic Interactions. There appear to be few previous studies of the mechanisms of ligand substitution reactions of (η^6-arene)Ru complexes. Reactions of aqua Ru(arene) complexes with N7 of cGMP obey second-order kinetics and therefore appear to proceed via an associative pathway involving a seven-coordinate transition state.[63] The rates of reaction of $[(\eta^6\text{-arene})\text{Ru(II)(en)}(H_2O]^{2+}$ complexes (and chloro complexes) with cGMP depends markedly on the nature of the arene, decreasing by over an order of magnitude in the series: THA > Bip > DHA ≫ Cym > Ben (Figure 6 and Table 6).

(47) Fernández, R.; Melchart, M.; Habtemariam, A.; Hanson, I.; Parsons, S.; Sadler, P. J., unpublished results.
(48) Habtemariam, A.; Sadler, P. J.; Aird, R. E.; Cummings, J.; Jodrell, D. I., unpublished results.
(49) Additionally in some cases, we have detected dinuclear adducts formed through Ru−N7 or −N1 or −N3 and Ru−*O*(PO_3) chelation: Ru−*O*(PO_3)-GMP*N7*−Ru, Ru−*O*(PO_3)IMP*N1*−Ru and Ru−*O*(PO_3)TMP*N3*−Ru.
(50) (a) Bose, R. N.; Viola, R. E.; Cornelius, R. D. *J. Am. Chem. Soc.* **1984**, *106*, 3336−3343. (b) Bose, R. N.; Cornelius, R. D.; Viola, R. E. *Inorg. Chem.* **1985**, *24*, 3989−3996.
(51) Reily, M. D.; Marzilli, L. G., *J. Am. Chem. Soc.* **1986**, *108*, 8299−8300.
(52) Kuo, L. Y.; Kanatzidis, M. G.; Sabat, M.; Tipton, A. L.; Marks, T. J. *J. Am. Chem. Soc.* **1991**, *113*, 9027−9045.
(53) Koike, T.; Kimura, E. *J. Am. Chem. Soc.* **1991**, *113*, 8935−8941.
(54) Aoki, S.; Kimura, E. *J. Am. Chem. Soc.* **2000**, *122*, 4542−4548.
(55) Tanase, T.; Yun, J. W.; Lippard, S. J. *Inorg. Chem.* **1996**, *35*, 3585−3594.
(56) (a) Rodriguez-Bailey, V. M.; Clarke, M. J. *Inorg. Chem.* **1997**, *36*, 1611−1618. (b) Rodriguez-Bailey, V. M.; LaChance-Galang, K. J.; Doan, P. E.; Clarke, M. J. *Inorg. Chem.* **1997**, *36*, 1873−1883.
(57) (a) Alessio, E.; Xu, Y.; Cauci, S.; Mestroni, G.; Quadrifoglio, F.; Viglino, P.; Marzilli, L. G. *J. Am. Chem. Soc.* **1989**, *111*, 7068−7071. (b) Tian, Y.; Yang, P.; Li, Q.; Guo, M.; Zhao, M. *Polyhedron* **1997**, *16*, 1993−1998.
(58) Binding of Ru(II) to dianionic nucleotides mono-, di-, and tri-phosphates may occur rapidly inside cells at pH 7.4, but phosphate is readily displaced by G N7. Also the pH close to the surface of DNA is thought to be more acidic (as low as pH 4.5): Lamm, G.; Pack, G. R. *Proc. Natl. Acad. Sci. U.S.A.* **1990**, *87*, 9033−9036, and Ru(II) binding to mono-nucleotide phosphates will be weak at this pH due to phosphate protonation.
(59) (a) Davies, M. S.; Thomas, D. S.; Hegmans, A.; Berners-Price, S. J.; Farrell, N. *Inorg. Chem.* **2002**, *41*, 1101−1109. (b) Davies, M. S.; Berners-Price, S. J.; Hambley, T. W. *Inorg. Chem.* **2000**, *39*, 5603−5613. (c) Frey, U.; Ranford, J. D.; Sadler, P. J. *Inorg. Chem.* **1993**, *32*, 1333−1340. (d) Yamamoto, T.; Moriwaki, Y.; Takahashi, S.; Tsutsumi, Z.; Yamakita, J.-I.; Higashino, K. *Metabolism* **1997**, *46*, 1339−1342.
(60) (a) Marcelis, A. T. M.; Erkelens, C.; Reedijk, J. *Inorg. Chim. Acta*. **1984**, *91*, 129−135. (b) Elmroth, S. K. C.; Lippard, S. J. *J. Am. Chem. Soc.* **1994**, *116*, 3633−3634. (c) Kozelka, J.; Barre, G. *Chem. Eur. J.* **1997**, *3*, 1405−1409.
(61) Jennerwein, M.; Andrews, P. A. *Drug Metab. Dispos.* **1995**, *23*, 178−184.
(62) Hung, Y.; Kung, W.-J.; Taube, H. *Inorg. Chem.* **1981**, *20*, 457−463.
(63) Tobe, M. L.; Burgess, J. *Inorganic Reaction Mechanisms*, 1st ed.; Wesley: New York, 1999; pp 37 and 584.

There is no correlation between the rates of cGMP N7-binding and pK_a values of aqua Ru(arene) complexes.[64] The faster rates of reaction for $[(\eta^6\text{-arene})\text{Ru(II)(en)}(H_2O)]^{2+}$ complexes containing the large arene ligands THA, Bip and DHA[65] imply lower activation free energies ($\Delta G^{\ddagger}$) for formation of seven-coordinate transition states. A significant contribution to $\Delta G^{\ddagger}$ may arise from $\pi-\pi$ stacking of the arene and purine ring[12] in the transition state (negative $\Delta H^{\ddagger}$). Such an interaction is not possible for the *p*-cymene and benzene complexes. Arene-purine $\pi-\pi$ stacking may also result in a positive contribution to $\Delta S^{\ddagger}$ through desolvation of cGMP in the reaction transition state.

Hydrophobic interactions could produce a driving force for DNA binding. A recent analysis of free energy contributions to DNA binding suggests that intercalation of ethidium, propidium, daunorubicin, and adriamycin is driven by hydrophobic effects and van der Waals contacts within the intercalation site.[66] Studies of the interaction of thymine derivatives with zinc cyclen containing a pendant acridine show that acridine-thymine ring-stacking increases the affinity of Zn(II) for dT N3.[67] For many other reported metal agents, however, the presence of a rigid aromatic rings, e.g., quinoline in *trans*-[Pt(quinoline)(NH_3)-(9EtG)Cl]$^+$,[68] has been found to significantly retard the rate of N7-binding of 5′-GMP. In contrast, for the Ru(arene) complexes studied here, the flexibility of large arene ligands reduces the steric requirements and makes simultaneous arene-nucleobase stacking and N7-covalent binding compatible. Our initial investigations of reactions of calf-thymus DNA show that chloro Ru THA, DHA and Bip complexes bind to DNA faster than the Cym complex, and CD, LD experiments suggest that the larger arene rings (THA, DHA and Bip) are oriented on DNA in a manner compatible with intercalation.[38] The rate of DNA binding appears to be specifically enhanced by hydrophobic interactions between the arene and the purine base.

Conclusions

We have shown here that anticancer complexes of the type $[(\eta^6\text{-arene})\text{Ru(en)Cl}]^+$ are highly selective in their recognition of binding sites on nucleosides and nucleotides. This arises not only from the differences in basicity between the binding sites, but also from the demanding constraints imposed on the reactive monofunctional site in these pseudo-octahedral "piano-stool" Ru(II) arene complexes.

$\{(\eta^6\text{-arene})\text{Ru(en)}\}^{2+}$ complexes exhibit a remarkably high preference for binding to guanine N7. Such binding is stabilized by H-bonding between the C6O of G and NH of the en ligand.[12] The lack of binding to adenine can be attributed to unfavorable interactions between the C6 NH_2 group and Ru en NH_2. Such a repulsive interaction also occurs for G when Ru binds to N1, but, if this NH_2 group is absent, as in inosine derivatives, then a significant amount of binding to N1 is observed. Similarly, binding of Ru to N3 of C derivatives is weak due to the repulsive interaction with the C4 NH_2 group. Binding to N3 of T is significant, but was not competitive with binding to G N7 at neutral pH. It is clear that nucleobase site-selectivity is strongly related to interactions with the en NH_2 group which is attractive toward exocyclic carbonyl oxygens but repulsive toward exocyclic amino groups of nucleobases.

Reactions of the chloro Ru(II) arene complexes with nucleotides proceed via hydrolysis followed by rapid binding to the phosphate monoester group. In contrast, binding to the monoanionic phosphodiester group of nucleotides is weak and was not detected. Bound phosphate groups are then readily displaced by base nitrogens. Studies of the kinetics of binding of $[(\eta^6\text{-arene})\text{Ru(en)X}]^{n+}$ (X = H_2O, Cl) to cGMP suggested that arene-purine base-stacking plays a significant role in stabilizing the transition state in the associative substitution reactions. Reactions of complexes containing arenes (THA, Bip, and DHA) which can take part in $\pi-\pi$ stacking are up to an order of magnitude faster than those containing arenes which cannot (Cym, Ben). Such kinetic effects could play a role in the biological activity of this class of complexes.

These studies provide a basis for investigating the recognition of duplex DNA by octahedral arene Ru(II) complexes. We anticipate that it should be possible to enhance the discrimination of DNA base recognition by appropriate modification of the chelating ligand. By appropriate choice of arene it may also possible to achieve a high degree of selectivity via kinetic effects due to $\pi-\pi$ arene-base stacking interactions (intercalation). Dual mode G N7/intercalative binding may also induce novel structural distortions in duplex DNA, and hence, the recognition by DNA binding proteins and repair enzymes. Consideration of all these factors allow optimization of the design of this series of anticancer complexes.

Acknowledgment. We thank the CVCP (ORS Award for H.C.), EPSRC, ETF, Wolfson Foundation, Royal Society and Wellcome Trust for their support for this work, and our colleagues in EC COST D8 and D20, and in the Cancer Research UK Oncology Unit, Western General Hospital (Edinburgh), for stimulating discussions. We also thank Dr. Fuyi Wang, Dr. Juan Mareque, Dr. Abraha Habtemariam and Dr. Claudia Blindauer (University of Edinburgh) for helpful discussions and for comments on this script.

Supporting Information Available: Table S1 giving species distribution and N(7)/N(1) ratios for inosine and guanosine binding by $\{(\eta^6\text{-Bip})\text{Ru(en)}\}^{2+}$ at various pH values. Figures S1−S10 showing 2D [^{1}H, ^{15}N] HSQC NMR time course for reaction of $[(\eta^6\text{-Bip})\text{Ru}(^{15}\text{N-en})\text{Cl}]^+$ with 5′-GMP, ^{1}H and ^{31}P NMR spectra for reaction of $[(\eta^6\text{-Bip})\text{Ru(en)Cl}]^+$ with 5′-GMP in phosphate buffer, ^{31}P NMR spectra for reaction of $[(\eta^6\text{-Bip})\text{Ru(en)Cl}]^+$ with Na_2HPO_4, ^{1}H and ^{31}P NMR spectra for reaction of $[(\eta^6\text{-Bip})\text{Ru(en)Cl}]^+$ with 5′-AMP at various pH values and percentage of Ru-*O*(PO_3)AMP adduct as a function of pH, ^{1}H and ^{31}P NMR spectra for reaction of $[(\eta^6\text{-Bip})\text{Ru(en)Cl}]^+$ with 5′-CMP, 5′-TMP and thymidine, ^{1}H or ^{31}P NMR pH titration curves for reactions of Ru(Bip) with 5′-AMP, 5′-CMP,

(64) Hydroxo Ru(arene) species (Ru−OH) appear to be much less reactive than aqua Ru(arene) species (Ru−OH_2), but the pK_a values for these five aqua Ru(arene) complexes (ref 20) lie within a narrow range: 8.01 (Ru−THA), 7.89 (Ru−DHA), 7.71 (Ru−Bip), 8.25 (Ru−Cym, see Figure S10) and 7.9 (Ru−Ben, ref 62). Thus, at pH 7.0, aqua complexes should predominate for all these arene complexes.

(65) The slower rate of reaction of DHA compared to THA complexes, may arise from the difference in hinge-bending of the arene. In both the chloro and the aqua Ru(DHA) complexes, the tricyclic ring system of DHA is bent down towards the Ru−Cl(O) bond by ca. 40° (refs 12 and 20), which may impose a steric constraint on coordination of N7. For the Ru(THA) complexes, such a steric constraint would be smaller because the ring system is bent up away from Ru by ca. 7° (refs 12 and 20).

(66) Ren, J.; Jenkins, T. C.; Chaires, J. B. *Biochemistry* **2000**, *39*, 8439−8447.
(67) Shionoya, M.; Ikeda, T.; Kimura, E.; Shiro, M. *J. Am. Chem. Soc.* **1994**, *116*, 3848−3859.
(68) Bierbach, U.; Farrell, N. *Inorg. Chem*. **1997**, *36*, 3657−3665.

5′-TMP, and thymidine, Scientist model used to determine the rate constants given in Table 6, time dependence plots of species concentrations for reactions of aqua Ru(arene) with cGMP, ^{1}H NMR pH titration for determination of the pK_a (H_2O) value of $[(\eta^6\text{-Cym})\text{Ru(en)}(H_2O)]^{2+}$. This material is available free of charge via the Internet at http://pubs.acs.org.

JA027719M